Transcription promotes the interaction of the FAcilitates Chromatin Transactions (FACT) complex with nucleosomes in *S. cerevisiae*

Benjamin J.E. Martin, Adam T. Chruscicki, and LeAnn J. Howe*

Department of Biochemistry and Molecular Biology, 2350 Health Sciences Mall, University of British Columbia, Vancouver, B.C., Canada, V6T 1Z3.

Data accession numbers: GSE111426 and GSE110286

Running title: FACT targeting to active genes

Key words: FACT, Spt16, Pob3, nucleosome, chromatin, transcription

Corresponding author:
LeAnn Howe
Department of Biochemistry and Molecular Biology
University of British Columbia
2350 Health Sciences Mall
Vancouver, B.C., Canada
V6T 1Z3
Phone: (604) 822-6297
Email: ljhowe@mail.ubc.ca

ABSTRACT

The FACT (FAcilitates Chromatin Transactions) complex is enriched on highly expressed genes, where it facilitates transcription while maintaining chromatin structure. How it is targeted to these regions is unknown. In vitro, FACT binds destabilized nucleosomes, supporting the hypothesis that FACT is targeted to transcribed chromatin through recognition of RNA polymerase-disrupted nucleosomes. In this study, we used high resolution analysis of FACT occupancy in *S. cerevisiae* to test this hypothesis. We demonstrate that FACT interacts with unstable nucleosomes *in vivo* and its interaction with chromatin is dependent on transcription by any of the three RNA polymerases. Deep sequencing of micrococcal nuclease-resistant fragments shows that FACT-bound nucleosomes exhibit differences in micrococcal nuclease sensitivity compared to bulk chromatin, consistent with a modified nucleosome structure being the preferred ligand for this complex. While the presence of altered nucleosomes associated with FACT can also be explained by the known ability of this complex to modulate nucleosome structure, transcription inhibition alleviates this effect indicating that it is not due to FACT interaction alone. Collectively these results suggest that FACT is targeted to transcribed genes through preferential interaction with RNA polymerase disrupted nucleosomes.

INTRODUCTION

FACT (FAcilitates Chromatin Transactions) is an abundant and conserved complex that promotes DNA-dependent processes, such as transcription and DNA replication. In animals and plants, FACT is comprised of the subunits, Spt16 and SSRP1, while in *S. cerevisiae*, the role of SSRP1 is performed by two proteins, Pob3 and Nhp6 (ORPHANIDES *et al.* 1999; BREWSTER *et al.* 2001; FORMOSA *et al.* 2001). FACT was originally identified through its ability to promote transcription elongation on a chromatin template in vitro (ORPHANIDES *et al.* 1998). It was later shown to enhance TBP binding at nucleosomal sites and promote histone displacement from the promoters of inducible genes (MASON AND STRUHL 2003; BISWAS *et al.* 2005). Consistent with these observations, yeast FACT (yFACT) destabilizes nucleosomes in vitro (FORMOSA *et al.* 2001; RHOADES *et al.* 2004; XIN *et al.* 2009; VALIEVA *et al.* 2016). Contrary to these data however, FACT has also been implicated in the stabilization of chromatin. In yeast, mutation of FACT subunits results in transcription initiation from cryptic sites within the bodies of genes, enhanced histone turnover, and a failure to re-establish chromatin following transcriptional repression (JAMAI *et al.* 2009; FORMOSA 2012; HAINER *et al.* 2012; VOTH *et al.* 2014). The seemingly opposing functions of FACT in both disrupting and stabilizing chromatin have been reconciled in a model in which FACT binds nucleosomes and maintains an altered nucleosome structure that allows RNA polymerase II (RNAPII) passage without histone loss (FORMOSA 2012).

FACT shows increased occupancy on highly expressed genes (MAYER *et al.* 2010; FENG *et al.* 2016; PATHAK *et al.* 2018), and is targeted with RNAPII upon gene induction in both flies and budding yeast (MASON AND STRUHL 2003; SAUNDERS *et al.*

2003; DUINA *et al.* 2007; NGUYEN *et al.* 2013; VINAYACHANDRAN *et al.* 2018). An unresolved question however, is how FACT is targeted to these regions. FACT interacts with multiple components of the transcription machinery, including RNA polymerases, the Paf1 complex, the chromatin remodeler, Chd1, and Cet1, a subunit of the capping enzyme, but whether any of these factors are required for global FACT occupancy has not been tested (KROGAN *et al.* 2002; SQUAZZO *et al.* 2002; SIMIC *et al.* 2003; TARDIFF *et al.* 2007; SEN *et al.* 2017). Moreover, various lines of evidence suggest that the recruitment of FACT may not be through direct interaction with the RNAPII transcriptional machinery. First, the timing of RNAPII and FACT recruitment to induced genes during heat shock differs (VINAYACHANDRAN *et al.* 2018). Second, FACT is also found at regions transcribed by RNAPI and III (BIRCH *et al.* 2009; TESSARZ *et al.* 2014). Finally, histone mutants cause delocalization of FACT independently of RNAPII and other elongation factors (DUINA *et al.* 2007; LLOYD *et al.* 2009; NGUYEN *et al.* 2013; PATHAK *et al.* 2018). Together, these data suggest that FACT is directed to transcribed regions through an indirect mechanism.

Several studies have demonstrated the interaction of FACT with nucleosomes in vitro, but only in the presence of a destabilizing stress. First, the HMG box protein, Nhp6, promotes the interaction of both human and yeast FACT with nucleosomes (FORMOSA *et al.* 2001; RUONE *et al.* 2003; RHOADES *et al.* 2004; ZHENG *et al.* 2014; VALIEVA *et al.* 2016; MCCULLOUGH *et al.* 2018). Like other HMG box proteins, Nhp6 weakens histone-DNA contacts, potentially "priming" nucleosomes for FACT binding (TRAVERS 2003; HEPP *et al.* 2017). Second, the introduction of a DNA double strand break promotes FACT binding to nucleosomes in vitro (TSUNAKA *et al.* 2016). Third, curaxins, a class of

drugs that promote unwrapping of nucleosomal DNA in vitro, "trap" FACT on chromatin (GASPARIAN *et al.* 2011; SAFINA *et al.* 2017; NESHER *et al.* 2018). Fourth, FACT binds hexasomes, made up of DNA, a H3-H3 tetramer and a single H2A-H2B dimer, but not nucleosomes (WANG *et al.* 2018). Finally, FACT is enriched in regions experiencing torsional stress (SAFINA *et al.* 2017), a force disruptive to nucleosomes (TEVES AND HENIKOFF 2014). These data, along with the disruptive effect of transcription on nucleosome structure (KIREEVA *et al.* 2002; SCHWABISH AND STRUHL 2004; KULAEVA *et al.* 2010; SHEININ *et al.* 2013; CHANG *et al.* 2014), support the intriguing hypothesis that FACT is targeted through preferential interaction with RNAP-destabilized nucleosomes. In this study, we tested this hypothesis using high resolution analysis of FACT occupancy in yeast. We demonstrate that the interaction of FACT with chromatin is dependent on transcription by any of the three RNA polymerases. Further, we show that FACT binds nucleosomes in vivo, preferentially interacting with genes with high nucleosome turnover. FACT-associated nucleosomes show altered nuclease sensitivity compared to bulk chromatin, which is consistent with FACT's ability to modulate nucleosome structure, however the enhanced nucleus sensitivity is partially independent of transcription, suggesting that it is not due to FACT binding per se. Instead, these data support the model that FACT is targeted to transcribed regions through preferential interaction with RNA polymerase-destabilized nucleosomes.

RESULTS

Transcription promotes the interaction of FACT with chromatin

To identify pathways for targeting FACT to transcribed regions, we first sought to confirm co-localization of FACT with RNAPII. To this end, we performed ChIP-seq of HA-tagged Spt16 and the RNAPII subunit, Rpb3, from the same whole cell extracts with two independent biological replicates. As FACT undergoes a dramatic redistribution during S-phase (FOLTMAN *et al.* 2013), we synchronized cells in G1 with α-factor. Our Spt16 ChIP-seq data agreed well with previously published FACT ChIP-seq experiments (Figure S1), and we observed a specific and striking co-localization of Spt16, but not an untagged control, with Rpb3 at individual loci (Figure 1A) and genome-wide (Figure 1B). In agreement with previous reports (MASON AND STRUHL 2003; MAYER *et al.* 2010; LIU *et al.* 2017; PATHAK *et al.* 2018), we found FACT enriched over the bodies of transcribed genes (Figure 1C), with binding primarily occurring downstream of the +1 nucleosome.

To determine whether transcription promotes FACT binding genome-wide, we first analyzed previously published data mapping RNAPII and Spt16 following depletion of Kin28, a kinase that facilitates promoter escape, using the rapamycin mediated "anchor away" technique (WONG *et al.* 2014). It should be noted that this analysis was conducted in cells grown in minimal media, which results in the previously observed, albeit unexplained, shift of RNAPII occupancy from the TSS to mid-gene when compared to cells grown in rich media (WARFIELD *et al.* 2017). Kin28 depletion results in a 5' shift of both Rpb3 and Spt16, as well as loss of both proteins over gene bodies (Figures 2A and S2), consistent with targeting of FACT by transcription. This shift of FACT localization was not commented on previously, perhaps because the authors focused on a small subset

of genes (WONG *et al.* 2014), but the 5' shift of FACT upon Kin28 depletion appears as a general effect across the 5521 genes analyzed here.

To more directly test whether FACT requires RNAPII for binding to transcribed genes we next treated cells with the general transcription inhibitor 1,10-phenanthroline monohydrate (1,10-pt) (GRIGULL *et al.* 2004) and analyzed Spt16 and RNAPII occupancy by ChIP-seq. Importantly, "spike-in" DNA controls were added immediately following DNA elution to normalize the number of DNA fragments recovered from treated to untreated cells (CHEN *et al.* 2015). Although the mechanism of action of 1,10-pt is not fully understood, short treatment (15 minutes) resulted in depletion of RNAPII across gene bodies, with the greatest effect over the 5' regions (Figures 2B and C). Similar to RNAPII, treatment of cells with 1,10-pt also depleted Spt16 from gene bodies and shifted Spt16 occupancy from 5' to 3' genic regions at both highly and poorly transcribed genes (Figures 2B-D), indicating that the interaction of FACT with DNA requires transcription. Supporting a strong dependence of FACT targeting on RNAPII, the changes in Spt16 and Rpb3 occupancy upon transcription inhibition were highly correlated genome-wide (Figure S3). Collectively, these results demonstrate that FACT targeting to transcribed regions occurs as a consequence of RNA polymerase activity.

While the above data is consistent with a model in which FACT is targeted through physical interaction with the RNAPII transcriptional machinery, several contradictions with this model exist. First, although FACT and RNAPII levels tightly correlated across gene bodies, poorly expressed genes exhibited higher binding of Spt16 relative to RNAPII than highly expressed genes (Figure 2D). This observation is better visualized in Figure S4A, which compares the ratio of Spt16 to Rpb3 with Rpb3 levels.

Such enrichment at poorly expressed genes was not observed for Spt5, an elongation factor that interacts directly with RNAPII (Figure S4B). Second, following transcription inhibition, the magnitude of Spt16 depletion was less than for Rpb3, even at 5' genic regions where Rpb3 depletion is most evident (Figure 2B), suggesting that FACT remains transiently associated with chromatin following RNAPII passage. Third, the length of DNA fragments co-precipitating with Spt16 and Rpb3 differed markedly (Figure S5A), with Rpb3-associated DNA being smaller than that associated with Spt16. Notably, the differences in fragment sizes were observed at both lowly and highly transcribed regions of the genome and across gene bodies (Figure S5B and C), confirming that the differences in fragment size are occurring at regions of co-localization, at least as observed across a population of cells. The differences in fragment sizes are unlikely due to technical variation in sample treatment as these ChIPs were performed from the same cell extracts, the DNA purifications and sequencing libraries were prepared in parallel, and the libraries were indexed, pooled, and sequenced together. Instead, the differences in DNA fragment size likely indicate that the majority of Rpb3 and Spt16 do not purify as a single nucleoprotein complex. Finally, transcription inhibition also resulted in depletion of FACT from RNAPI and III-transcribed regions (Figures S6, S7 and S8). Collectively, these data support a model whereby transcription promotes the interaction of FACT with chromatin via an indirect mechanism.

FACT binds polymerase-destabilized nucleosomes in vivo

FACT binds disrupted nucleosomes in vitro (FORMOSA *et al.* 2001; RUONE *et al.* 2003; ZHENG *et al.* 2014; TSUNAKA *et al.* 2016; MCCULLOUGH *et al.* 2018; NESHER *et al.*

2018; WANG *et al.* 2018), supporting the hypothesis that it is targeted to transcribed genes through interaction with RNA polymerase-destabilized nucleosomes. To confirm that FACT binds nucleosomes in vivo, we purified FACT via a TAP tag on Pob3. Figure 3A shows that FACT co-purified with stoichiometric levels of histones H2A, H2B, H3 and H4. Immunoprecipitation of H2B from purified FACT co-precipitated all four core histones (Figure 3B), indicating that FACT interacts with intact histone octamers as opposed to select histone pairs. To test whether these histones were nucleosomal, we ChIPped HA-tagged Spt16 from MNase-treated extracts prepared from formaldehyde cross-linked cells. The co-purifying DNA was subjected to paired-end sequencing and a heatmap showing the location of sequence reads across genes sorted by RNAPII occupancy showed that the positioning of FACT-associated DNA closely matched that of input nucleosomes (Figure 3C). This is more evident in Figure S9, in which the total number of sequence fragments recovered were normalized between genes to compensate for increased Spt16 occupancy at highly expressed genes. Despite the similarities between input and FACT-bound chromatin, noticeable differences were observed including increased recovery of sequence fragments from highly expressed genes, depletion and shift of the +1 nucleosome peak, and enrichment of FACT over gene bodies (Figure 3D). Thus, despite the reported inability of FACT to bind nucleosomes in the absence of destabilizing stress in vitro (TSUNAKA *et al.* 2009; WANG *et al.* 2018), our results suggest that FACT can bind nucleosomes on transcribed genes in vivo.

We next asked whether FACT preferentially interacts with unstable nucleosomes. One hallmark of unstable nucleosomes is increased histone turnover, and indeed, Spt16 occupancy correlated with replication independent (RI) histone turnover (Figure 4A,

Spearman rank correlation coefficient of 0.47) (DION *et al.* 2007). Histone loss is also associated with high levels of transcription, so to test if FACT correlated with histone turnover independently of RNAPII-levels, we employed a technique called partial correlation, a statistical method that calculates the association between two factors after eliminating the effects of other variables (KIM 2015). Importantly, this technique allows estimation of the direct interaction between two factors while controlling for a confounding variable. Partial correlation analysis revealed that RI histone turnover over gene bodies directly correlated with Spt16 and not Rpb3 (Figure 4A), demonstrating that FACT co-localizes with RI histone turnover independently of transcription. To assess this relationship another way, we ordered genes by Rpb3 occupancy, and in a sliding window of 500 genes assessed the mean level of RI histone turnover for the 100 genes with the highest or lowest Spt16 occupancy relative to Rpb3 (Figure 4B). Aside from very highly transcribed genes, we found RI histone turnover increased at genes with higher Spt16 relative to Rpb3 occupancy (Figure 4C). Although we cannot rule out the possibility that the link between Spt16 occupancy and histone turnover is due to FACT promoting RI histone turnover, the demonstrated ability of FACT to suppress histone turnover *in vivo* argues that this is not the case (JAMAI *et al.* 2009). Indeed, analyzing published MNase-seq data in *spt16* mutant cells (TRUE *et al.* 2016) revealed that FACT inactivation leads to preferential loss of nucleosomes at these genes (Figure 4D), supporting a model whereby FACT preferentially binds to regions of destabilized nucleosomes where it acts to stabilize chromatin.

The use of paired-end sequencing in our analyses afforded us the opportunity to examine the nuclease sensitivity, and thus potential alterations, of FACT-bound

nucleosomes. While FACT-associated DNA exhibited resistance to MNase, consistent with the binding of nucleosomes, specific alterations from bulk chromatin were observed (Figure 5A). FACT-bound DNA fragments, but not those from an untagged control, exhibited increased levels of longer (200 - 260 bp) and shorter (100 - 130 bp) than mononucleosome sized (140 - 160 bp) fragments. These differences were unlikely to have arisen from technical variation in sample processing as the ChIPs and inputs were processed in parallel, indexed, and pooled together for sequencing. To determine where the altered, FACT-bound nucleosomes were located, we used two-dimensional occupancy plots to visualize the boundaries of MNase-resistant fragments associated with FACT or with bulk chromatin, relative to the +1 nucleosomes of RNAPII transcribed genes. Shown in Figure 5C, these plots simultaneously display DNA sequencing data as: 1) a heatmap of the total counts of the left (left panels) and right (right panels) boundaries of MNase protection (as designated in Figure 5B), 2) the total length of the MNase-resistant fragments (Y-axis) and 3) position of the boundary relative to the dyad of the +1 nucleosomes of 5521 genes (X-axis). Analysis of bulk chromatin showed peaks of left boundary signal at ~-75 bp and right boundary signal at ~+75 bp relative to +1 nucleosomes on the X-axis and ~150 bp on the Y-axis, consistent with well positioned, +1 mononucleosomes protecting ~150 bp of DNA (Figure 5C, top panels). Also evident, albeit fainter, was a ~-75 bp left boundary signal and a ~+250 bp right boundary signal at ~315 bp on the Y-axis, indicative of di-nucleosomes containing both the +1 and +2 nucleosomes. Of additional note, signals were also observed below 150 bp on the Y-axis, that slope toward the nucleosome dyads. MNase preferentially digests linker DNA, but transient unwrapping of DNA from the octamer surface can result in “chewing” of the

DNA ends. Thus, these lower signals likely represent MNase trimming of nucleosomes from either direction.

Performing 2D analysis of DNA fragment boundaries from FACT-associated nucleosomes revealed many differences from bulk nucleosomes (Figure 5C, lower panels). First, nucleosomes bound to FACT showed an increased proportion of "trimmed" nucleosomes. These smaller fragments could also represent hexasomes, reported to protect ~110 bp from MNase (ARIMURA *et al.* 2012), as FACT has been shown to form a ternary complex with a single dimer of histones H2A-H2B and a H3-H4 tetramer in vitro (WANG *et al.* 2018). Interestingly, equivalent MNase trimming of Spt16-bound fragments was observed on the promoter-proximal (left boundary) and promoter-distal (right boundary) edges of nucleosomes, suggesting that the direction of transcription had little impact on the presence of these "sub-nucleosomes".

Another interesting result from our 2D analysis is that discrete signals at 315 bp, representative of di-nucleosomes, were less evident in FACT-associated DNA. Instead, a continuum of fragment sizes from mono to di-nucleosomes was observed, suggesting that FACT can alter typical spacing between nucleosomes. Indeed, DNA fragments in the 200 to 260 bp range could be indicative of "overlapping di-nucleosomes". Such structures, composed of a hexasome and a nucleosome, have been demonstrated in vitro by many labs (ULYANOVA AND SCHNITZLER 2005; ENGEHOLM *et al.* 2009; KATO *et al.* 2017), and indeed, the susceptibility of FACT-associated nucleosomes to lose an H2A/H2B dimer (BELOTSERKOVSKAYA *et al.* 2003) may make these nucleosomes more prone to forming such structures. Consistent with this, Figure 5A shows that FACT-bound nucleosomes were depleted in the canonical di-nucleosome signal observed in total chromatin.

While, the altered nuclease sensitivity of Spt16-bound nucleosomes is consistent with a preference of FACT for transcription-disrupted nucleosomes, FACT is also reported to alter nucleosome structure *in vitro* (McCullough et al., 2018; Xin et al., 2009), and thus a modified nucleosome structure could also be a consequence of FACT binding. To differentiate between these two possibilities, we rationalized that, if FACT modifies nucleosome structure on its own, then the altered pattern of digestion should be independent of the destabilizing stress of transcription. To test this, we divided input and Spt16 ChIP DNA fragments into three bins [100-130 bp (purple lines), 140-160 bp (teal lines) and 200-260 bp (orange lines)] and plotted the abundance of each relative to the +1 nucleosomes of highly expressed genes (dark lines) and poorly expressed genes (light lines) (Figure 6). This analysis revealed Spt16 co-precipitated increased amounts of shorter (100 – 130 bp) and longer (200 – 260 bp) sized DNA fragments from highly expressed genes compared to poorly expressed genes. Interestingly, the major species of larger FACT-bound fragments predominantly occurred upstream and overlapping the +2 NCP, suggesting that the +1 NCP has shifted downstream to create an overlapping di-nucleosome of the +1 and +2 NCPs. The increased levels of alternate fragments at highly expressed genes was diminished upon transcription inhibition. Collectively these results indicate that altered MNase sensitivity of FACT-bound nucleosomes is dependent on transcription, suggesting that nucleosome disruption is primarily a cause as opposed to consequence of FACT binding. These data are consistent with a model in which FACT is targeted to active genes through preferential interaction with RNAP-disrupted nucleosomes.

DISCUSSION

In this study, we show that the FACT complex binds nucleosomes in vivo and is recruited to chromatin as a consequence of transcription by any of the three RNA polymerases. These data, together with extensive evidence that FACT binds destabilized nucleosomes in vitro, are consistent with a model in which FACT is targeted to transcribed regions through preferential interaction with RNAP-destabilized nucleosomes. Individual domains of FACT subunits have been shown to bind DNA and all four core histones in vitro (STUWE *et al.* 2008; VANDEMARK *et al.* 2008; WINKLER *et al.* 2011; HONDELE *et al.* 2013; KEMBLE *et al.* 2013; HOFFMANN AND NEUMANN 2015; KEMBLE *et al.* 2015; TSUNAKA *et al.* 2016). The unwrapping of nucleosomal DNA by RNA polymerases could reveal high affinity binding sites that stabilize the binding of FACT at transcribed genes.

Our results show that Spt16-associated nucleosomes exhibit altered sensitivity to MNase, which is indicative to FACT binding to atypical nucleosome structures, including potentially overlapping di-nucleosomes. While the function of overlapping di-nucleosomes has not been investigated (LOWARY AND WIDOM 1998; ULYANOVA AND SCHNITZLER 2005; ENGEHOLM *et al.* 2009; KATO *et al.* 2017), one possibility may be to increase nucleosome mobility on transcribed genes. Nucleosomes restrict the movement of their neighbors (KORNBERG AND STRYER 1988; ZHANG *et al.* 2011), but facilitating formation of overlapping nucleosomes would increase flexibility of movement without the need for octamer eviction, which coincides with the ability of FACT to both promote transcription while stabilizing chromatin structure. The altered sensitivity of FACT-associated nucleosomes is largely dependent on active transcription, which is consistent

with it being a cause, as opposed to a consequence of FACT binding. However, it should be noted that multiple studies have shown that FACT can disrupt nucleosome structure in vitro (XIN *et al.* 2009; VALIEVA *et al.* 2016), and thus we cannot rule out the possibility that FACT further alters chromatin structure once bound.

In addition to functioning in transcription, FACT plays an essential role in DNA replication. During S phase, FACT relocates to newly replicated chromatin (FOLTMAN *et al.* 2013; ALABERT *et al.* 2014), where it interacts with multiple components of the replication machinery (WITTMEYER AND FORMOSA 1997; GAMBUS *et al.* 2006; VANDEMARK *et al.* 2006). Moreover, mutation of FACT results in sensitivity to hydroxyurea (HU), delayed S phase progression (SCHLESINGER AND FORMOSA 2000; HERRERA-MOYANO *et al.* 2014) and defects in chromatin assembly on nascent DNA (YANG *et al.* 2016). Finally, mutation of FACT results in dependence on the S phase checkpoint for viability (SCHLESINGER AND FORMOSA 2000). However, despite extensive data supporting a requirement for FACT in DNA replication, its actual function in this process is unclear. Part of this mystery is routed in confusion over the molecular function of FACT. While FACT was originally proposed to be a histone chaperone that deposits free histones on DNA (BELOTSERKOVSKAYA *et al.* 2003), data overwhelmingly suggests that FACT instead binds intact nucleosomes (RUONE *et al.* 2003; TSUNAKA *et al.* 2009; XIN *et al.* 2009; WINKLER *et al.* 2011; TSUNAKA *et al.* 2016; VALIEVA *et al.* 2016; VALIEVA *et al.* 2017). Chromatin assembled on newly replicated DNA undergoes a maturation step shortly following DNA replication (FENNESSY AND OWEN-HUGHES 2016; VASSEUR *et al.* 2016), raising the possibility that FACT recognizes newly formed,

unstable nucleosomes on nascent DNA, and akin to its role in transcription, stabilizes these nucleosomes until maturity.

MATERIALS AND METHODS

Yeast strains and antibodies

All strains used in this study were isogenic to S288C. The Pob3TAP and Spt16HA$_6$ were derived from FY602 (*MATa his3Δ200 lys2-128δ leu2Δ1 trp1Δ63 ura3-52*), a generous gift of Fred Winston. Yeast culture, genetic manipulations, and strain verification were performed using standard protocols. Antibodies used were from Roche [11 583 816 001 (HA)], Biolegend [665004 (Rpb3)], Active Motif [39237 (histone H2B)], and Millipore [PP64 (IgG)].

Spt16 Chromatin ImmunoPrecipitation (ChIP) sequencing

Yeast cells were arrested in G1 by treatment with 10 μM alpha factor for three hours (synchronization confirmed by inspection of cell morphology under the microscope). Transcription inhibition was performed by treatment with 400 μg/mL 1,10-pt for 15 minutes. Crosslinking was performed with 1% (vol/vol) formaldehyde for 15 minutes at room temperature and quenched with 125 mM glycine for 15 minutes.

Sonicated ChIP-seq was performed essentially as described previously (LAWRENCE *et al.* 2017). Briefly, cells were disrupted by bead beating, chromatin was sonicated to an average DNA length of 250 bp (Biorupter, Diagenode), and parallel immunoprecipitations were performed using α-HA or α-Rpb3 antibodies.

MNase ChIP-seq was performed essentially as described previously (MALTBY *et al.* 2012). Briefly, cells were disrupted by bead beating, chromatin was digested to mononucleosomes with MNase, and immunoprecipitations were performed using α-HA antibody. Sequencing libraries were prepared as described previously (MALTBY *et al.* 2012; MARTIN *et al.* 2017). Exogenous DNA spike-ins were added to ChIP-seq eluates () in order for quantification of global changes in IP efficiency.

Sequencing libraries were prepared essentially as described previously (MALTBY *et al.* 2012). Briefly, 2 ng of IP or input material was end-repaired, A-tailed, and adapters ligated, before PCR amplification with indexed primers. We performed 10 and 11 rounds of PCR amplification for MNase and sonication ChIP-seq experiments respectively. All DNA purification steps used SPRI beads. Samples were pooled, gel-purified (50 bp - 600 bp region) and sequenced on an Illumina HiSeq 2500.

Data analysis

Sequenced reads were trimmed for adapter sequences using cutadapt (http://cutadapt.readthedocs.io/en/stable/). Trimmed reads were then aligned to the Saccer3 genome using bowtie2 (LANGMEAD AND SALZBERG 2012), and filtered for paired reads with a mapping quality of at least 5 using SAMtools (LI *et al.* 2009)). Fragments mapping to synthetic spike in sequences were used to scale ChIP-seq datasets following 1,10-pt transcription inhibition. Reads Per Genome Coverage (RPGC) bigwig tracks were generated using deeptools (RAMIREZ *et al.* 2014; RAMIREZ *et al.* 2016). Size selected Counts Per Million Fragments (CPMF) tracks were generated using a custom bash script using AWK, the BEDtools (QUINLAN AND HALL 2010), and the UCSC bedgraphtobigwig

function (KENT *et al.* 2010). Genome browser shots were generated using the UCSC genome browser (KENT *et al.* 2002).

Genome wide coverage in genome wide windows for ChIP-seq data was generated using deeptools, and heatmaps and scatter plots were plotted in R using pheatmap and smoothscatter functions respectively. Fragment length histograms were plotted in R, and fragments overlapping specific genomic regions were selected for using BEDtools. Coverage heatmaps were generated using deeptools. For average plots and row-normalized heatmaps, feature-aligned matrixes were constructed using deeptools and plots were then generated in R using base plots or pheatmap functions respectively. For average plots, to avoid effects due to varying gene lengths, plots only include data until the TTS, with the fraction of genes plotted at a given position indicated by a grey line. The MNase 2D heatmaps were generated using AWK and BEDtools, with the final heatmaps were plotted in R using pheatmap.

For gene body comparisons of Rpb3 and Spt16, gene bodies were defined as +73 bp downstream of the +1 dyad, to avoid initiation effects, to the TTS. To avoid gene-length effects, only genes (+1 dyad to TSS) longer than 500 bp were analyzed, but similar results were seen across all gene lengths. ChIP-seq fragments overlapping gene bodies were counted per million fragments and scatter plots generated using the SmoothScatter function in R. Partial correlations were calculated using the ppcor function in R (KIM 2015). For histone turnover data (DION *et al.* 2007), average values over gene bodies were calculated using the java genomics toolkit (https://github.com/timpalpant/java-genomics-toolkit). For MNase-seq data from Wildtype and *spt16-197* strains, DNA fragments (TRUE *et al.* 2016) overlapping gene bodies were counted per million

fragments. For gene windows, genes were ordered by Rpb3 levels in a 500-gene sliding window. For each window the top and bottom 100 genes for Spt16 minus Rpb3 were selected and the mean value plotted. The 95% confidence interval was bootstrapped and plotted as the shaded area in the graph. Colour schemes were generated using the RColorBrewer Package in R.

Published datasets:

For histone turnover data (DION *et al.* 2007), probe intensity values were converted to Saccer3 using the UCSC liftover tool and conversion to wig format, linear interpolation to a maximum of 500 bp, and average values over gene bodies were calculated using the java genomics toolkit (https://github.com/timpalpant/java-genomics-toolkit). Wildtype and *spt16-197* MNase-seq datasets (TRUE *et al.* 2016) were downloaded from SRA project SRP073244. Spt16 ChIP-seq datasets were downloaded from SRA projects SRP055441 (FENG *et al.* 2016), SRP018874 (FOLTMAN *et al.* 2013), SRP073244 (TRUE *et al.* 2016), SRP036647 (WONG *et al.* 2014). The Spt16 ChIP-exo dataset was downloaded from SRA project SRP106497 (VINAYACHANDRAN *et al.* 2018). Spt5 and Rpb1 ChIP-seq datasets (BAEJEN *et al.* 2017) were downloaded from SRP071780. Sequenced reads were processed as described above.

Transcription Start Site (TSS) annotations are from Park et al (PARK AND LUGER 2008). Plus One Nucleosome and Transcription Termination Site (TTS) are from (CHEREJI *et al.* 2018). Yeast genome features were downloaded from http://www.yeastgenome.org/

FACT purification

Pob3TAP and its associated proteins were purified from one litre of yeast cells as described (LAMBERT *et al.* 2009). For micrococcal nuclease digestion, magnetic beads containing purified FACT-nucleosome complexes were washed in 50 mM Tris pH 8, 4 mM $MgCl_2$, 2 mM $CaCl_2$ and digested with increasing amounts of nuclease. Reactions were stopped by washing the beads in 50 mM Tris pH 8, 4 mM $MgCl_2$, 10 mM EDTA and the DNA was purified using phenol:chloroform:isoamyl alcohol extraction followed by ethanol precipitation.

Data availability

Strains and plasmids are available upon request. The ChIP-seq data generated for this study have been deposited in the Gene Expression Omnibus (GEO) database under accession numbers GSE111426 and GSE110286. Supplementary figures have been uploaded to figshare.

Acknowledgments

We acknowledge Tim Formosa for his constructive feedback. This work was supported by a Natural Sciences and Engineering Research Council (NSERC) Discovery Grant awarded to L.J.H. B.J.E.M was supported by graduate student fellowships from NSERC.

REFERENCES

Alabert, C., J. C. Bukowski-Wills, S. B. Lee, G. Kustatscher, K. Nakamura *et al.*, 2014 Nascent chromatin capture proteomics determines chromatin dynamics during DNA replication and identifies unknown fork components. Nat Cell Biol 16**:** 281-293.

Arimura, Y., H. Tachiwana, T. Oda, M. Sato and H. Kurumizaka, 2012 Structural analysis of the hexasome, lacking one histone H2A/H2B dimer from the conventional nucleosome. Biochemistry 51**:** 3302-3309.

Baejen, C., J. Andreani, P. Torkler, S. Battaglia, B. Schwalb *et al.*, 2017 Genome-wide Analysis of RNA Polymerase II Termination at Protein-Coding Genes. Mol Cell.

Belotserkovskaya, R., S. Oh, V. A. Bondarenko, G. Orphanides, V. M. Studitsky *et al.*, 2003 FACT facilitates transcription-dependent nucleosome alteration. Science 301**:** 1090-1093.

Birch, J. L., B. C. Tan, K. I. Panov, T. B. Panova, J. S. Andersen *et al.*, 2009 FACT facilitates chromatin transcription by RNA polymerases I and III. EMBO J 28**:** 854-865.

Biswas, D., Y. Yu, M. Prall, T. Formosa and D. J. Stillman, 2005 The yeast FACT complex has a role in transcriptional initiation. Mol Cell Biol 25**:** 5812-5822.

Brewster, N. K., G. C. Johnston and R. A. Singer, 2001 A bipartite yeast SSRP1 analog comprised of Pob3 and Nhp6 proteins modulates transcription. Mol Cell Biol 21**:** 3491-3502.

Chang, H. W., O. I. Kulaeva, A. K. Shaytan, M. Kibanov, K. Kuznedelov *et al.*, 2014 Analysis of the mechanism of nucleosome survival during transcription. Nucleic Acids Res 42**:** 1619-1627.

Chen, K., Z. Hu, Z. Xia, D. Zhao, W. Li *et al.*, 2015 The Overlooked Fact: Fundamental Need for Spike-In Control for Virtually All Genome-Wide Analyses. Mol Cell Biol 36**:** 662-667.

Chereji, R. V., S. Ramachandran, T. D. Bryson and S. Henikoff, 2018 Precise genome-wide mapping of single nucleosomes and linkers in vivo. Genome Biol 19**:** 19.

Dion, M. F., T. Kaplan, M. Kim, S. Buratowski, N. Friedman *et al.*, 2007 Dynamics of replication-independent histone turnover in budding yeast. Science 315**:** 1405-1408.

Duina, A. A., A. Rufiange, J. Bracey, J. Hall, A. Nourani *et al.*, 2007 Evidence that the localization of the elongation factor Spt16 across transcribed genes is dependent upon histone H3 integrity in Saccharomyces cerevisiae. Genetics 177**:** 101-112.

Engeholm, M., M. de Jager, A. Flaus, R. Brenk, J. van Noort *et al.*, 2009 Nucleosomes can invade DNA territories occupied by their neighbors. Nat Struct Mol Biol 16**:** 151-158.

Feng, J., H. Gan, M. L. Eaton, H. Zhou, S. Li *et al.*, 2016 Non-coding transcription is a driving force for nucleosome instability in spt16 mutant cells. Mol Cell Biol.

Fennessy, R. T., and T. Owen-Hughes, 2016 Establishment of a promoter-based chromatin architecture on recently replicated DNA can accommodate variable inter-nucleosome spacing. Nucleic Acids Res.

Foltman, M., C. Evrin, G. De Piccoli, R. C. Jones, R. D. Edmondson *et al.*, 2013 Eukaryotic replisome components cooperate to process histones during chromosome replication. Cell Rep 3**:** 892-904.

Formosa, T., 2012 The role of FACT in making and breaking nucleosomes. Biochim Biophys Acta 1819**:** 247-255.

Formosa, T., P. Eriksson, J. Wittmeyer, J. Ginn, Y. Yu *et al.*, 2001 Spt16-Pob3 and the HMG protein Nhp6 combine to form the nucleosome-binding factor SPN. EMBO J 20**:** 3506-3517.

Gambus, A., R. C. Jones, A. Sanchez-Diaz, M. Kanemaki, F. van Deursen *et al.*, 2006 GINS maintains association of Cdc45 with MCM in replisome progression complexes at eukaryotic DNA replication forks. Nat Cell Biol 8**:** 358-366.

Gasparian, A. V., C. A. Burkhart, A. A. Purmal, L. Brodsky, M. Pal *et al.*, 2011 Curaxins: anticancer compounds that simultaneously suppress NF-kappaB and activate p53 by targeting FACT. Sci Transl Med 3**:** 95ra74.

Grigull, J., S. Mnaimneh, J. Pootoolal, M. D. Robinson and T. R. Hughes, 2004 Genome-wide analysis of mRNA stability using transcription inhibitors and microarrays reveals posttranscriptional control of ribosome biogenesis factors. Mol Cell Biol 24**:** 5534-5547.

Hainer, S. J., B. A. Charsar, S. B. Cohen and J. A. Martens, 2012 Identification of Mutant Versions of the Spt16 Histone Chaperone That Are Defective for Transcription-Coupled Nucleosome Occupancy in Saccharomyces cerevisiae. G3 (Bethesda) 2**:** 555-567.

Hepp, M. I., M. Smolle, C. Gidi, R. Amigo, N. Valenzuela *et al.*, 2017 Role of Nhp6 and Hmo1 in SWI/SNF occupancy and nucleosome landscape at gene regulatory regions. Biochim Biophys Acta 1860**:** 316-326.

Herrera-Moyano, E., X. Mergui, M. L. Garcia-Rubio, S. Barroso and A. Aguilera, 2014 The yeast and human FACT chromatin-reorganizing complexes solve R-loop-mediated transcription-replication conflicts. Genes Dev 28**:** 735-748.

Hoffmann, C., and H. Neumann, 2015 In vivo mapping of FACT-histone interactions identifies a role of Pob3 C-terminus in H2A-H2B binding. ACS Chem Biol.

Hondele, M., T. Stuwe, M. Hassler, F. Halbach, A. Bowman *et al.*, 2013 Structural basis of histone H2A-H2B recognition by the essential chaperone FACT. Nature 499**:** 111-114.

Jamai, A., A. Puglisi and M. Strubin, 2009 Histone chaperone spt16 promotes redeposition of the original h3-h4 histones evicted by elongating RNA polymerase. Mol Cell 35**:** 377-383.

Kato, D., A. Osakabe, Y. Arimura, Y. Mizukami, N. Horikoshi *et al.*, 2017 Crystal structure of the overlapping dinucleosome composed of hexasome and octasome. Science 356**:** 205-208.

Kemble, D. J., L. L. McCullough, F. G. Whitby, T. Formosa and C. P. Hill, 2015 FACT Disrupts Nucleosome Structure by Binding H2A-H2B with Conserved Peptide Motifs. Mol Cell 60**:** 294-306.

Kemble, D. J., F. G. Whitby, H. Robinson, L. L. McCullough, T. Formosa *et al.*, 2013 Structure of the Spt16 middle domain reveals functional features of the histone chaperone FACT. J Biol Chem 288**:** 10188-10194.

Kent, W. J., C. W. Sugnet, T. S. Furey, K. M. Roskin, T. H. Pringle *et al.*, 2002 The human genome browser at UCSC. Genome Res 12**:** 996-1006.

Kent, W. J., A. S. Zweig, G. Barber, A. S. Hinrichs and D. Karolchik, 2010 BigWig and BigBed: enabling browsing of large distributed datasets. Bioinformatics 26**:** 2204-2207.

Kim, S., 2015 ppcor: An R Package for a Fast Calculation to Semi-partial Correlation Coefficients. Commun Stat Appl Methods 22**:** 665-674.

Kireeva, M. L., W. Walter, V. Tchernajenko, V. Bondarenko, M. Kashlev *et al.*, 2002 Nucleosome remodeling induced by RNA polymerase II: loss of the H2A/H2B dimer during transcription. Mol Cell 9**:** 541-552.

Kornberg, R. D., and L. Stryer, 1988 Statistical distributions of nucleosomes: nonrandom locations by a stochastic mechanism. Nucleic Acids Res 16**:** 6677-6690.

Krogan, N. J., M. Kim, S. H. Ahn, G. Zhong, M. S. Kobor *et al.*, 2002 RNA polymerase II elongation factors of Saccharomyces cerevisiae: a targeted proteomics approach. Mol Cell Biol 22**:** 6979-6992.

Kulaeva, O. I., F. K. Hsieh and V. M. Studitsky, 2010 RNA polymerase complexes cooperate to relieve the nucleosomal barrier and evict histones. Proc Natl Acad Sci U S A 107**:** 11325-11330.

Lambert, J. P., L. Mitchell, A. Rudner, K. Baetz and D. Figeys, 2009 A novel proteomics approach for the discovery of chromatin-associated protein networks. Mol Cell Proteomics 8**:** 870-882.

Langmead, B., and S. L. Salzberg, 2012 Fast gapped-read alignment with Bowtie 2. Nat Methods 9**:** 357-359.

Lawrence, M. B. D., N. Coutin, J. K. Choi, B. J. E. Martin, N. A. T. Irwin *et al.*, 2017 Histone Acetylation, Not Stoichiometry, Regulates Linker Histone Binding in Saccharomyces cerevisiae. Genetics 207**:** 347-355.

Li, H., B. Handsaker, A. Wysoker, T. Fennell, J. Ruan *et al.*, 2009 The Sequence Alignment/Map format and SAMtools. Bioinformatics 25**:** 2078-2079.

Liu, S., Z. Xu, H. Leng, P. Zheng, J. Yang *et al.*, 2017 RPA binds histone H3-H4 and functions in DNA replication-coupled nucleosome assembly. Science 355**:** 415-420.

Lloyd, A., K. Pratt, E. Siebrasse, M. D. Moran and A. A. Duina, 2009 Uncoupling of the patterns of chromatin association of different transcription elongation factors by a histone H3 mutant in Saccharomyces cerevisiae. Eukaryot Cell 8**:** 257-260.

Lowary, P. T., and J. Widom, 1998 New DNA sequence rules for high affinity binding to histone octamer and sequence-directed nucleosome positioning. J Mol Biol 276**:** 19-42.

Maltby, V. E., B. J. E. Martin, J. Brind'Amour, A. T. Chruscicki, K. L. McBurney *et al.*, 2012 Histone H3K4 demethylation is negatively regulated by histone H3 acetylation in Saccharomyces cerevisiae. Proceedings of the National Academy of Sciences of the United States of America 109**:** 18505-18510.

Martin, B. J., K. L. McBurney, V. E. Maltby, K. N. Jensen, J. Brind'Amour *et al.*, 2017 Histone H3K4 and H3K36 Methylation Independently Recruit the NuA3

Histone Acetyltransferase in Saccharomyces cerevisiae. Genetics 205: 1113-1123.
Mason, P. B., and K. Struhl, 2003 The FACT Complex Travels with Elongating RNA Polymerase II and Is Important for the Fidelity of Transcriptional Initiation In Vivo. Molecular and Cellular Biology 23: 8323-8333.
Mayer, A., M. Lidschreiber, M. Siebert, K. Leike, J. Soding *et al.*, 2010 Uniform transitions of the general RNA polymerase II transcription complex. Nat Struct Mol Biol 17: 1272-1278.
McCullough, L. L., Z. Connell, H. Xin, V. M. Studitsky, A. V. Feofanov *et al.*, 2018 Functional roles of the DNA-binding HMGB domain in the histone chaperone FACT in nucleosome reorganization. J Biol Chem.
Nesher, E., A. Safina, I. Aljahdali, S. Portwood, E. S. Wang *et al.*, 2018 Role of chromatin damage and chromatin trapping of FACT in mediating the anticancer cytotoxicity of DNA-binding small molecule drugs. Cancer Res.
Nguyen, H. T., W. Wharton, 2nd, J. A. Harper, J. R. Dornhoffer and A. A. Duina, 2013 A nucleosomal region important for ensuring proper interactions between the transcription elongation factor Spt16 and transcribed genes in Saccharomyces cerevisiae. G3 (Bethesda) 3: 929-940.
Orphanides, G., G. LeRoy, C. H. Chang, D. S. Luse and D. Reinberg, 1998 FACT, a factor that facilitates transcript elongation through nucleosomes. Cell 92: 105-116.
Orphanides, G., W. H. Wu, W. S. Lane, M. Hampsey and D. Reinberg, 1999 The chromatin-specific transcription elongation factor FACT comprises human SPT16 and SSRP1 proteins. Nature 400: 284-288.
Park, Y. J., and K. Luger, 2008 Histone chaperones in nucleosome eviction and histone exchange. Curr Opin Struct Biol 18: 282-289.
Pathak, R., P. Singh, S. Ananthakrishnan, S. Adamczyk, O. Schimmel *et al.*, 2018 Acetylation-Dependent Recruitment of the FACT Complex and Its Role in Regulating Pol II Occupancy Genome-Wide in Saccharomyces cerevisiae. Genetics.
Quinlan, A. R., and I. M. Hall, 2010 BEDTools: a flexible suite of utilities for comparing genomic features. Bioinformatics 26: 841-842.
Ramirez, F., F. Dundar, S. Diehl, B. A. Gruning and T. Manke, 2014 deepTools: a flexible platform for exploring deep-sequencing data. Nucleic Acids Res 42: W187-191.
Ramirez, F., D. P. Ryan, B. Gruning, V. Bhardwaj, F. Kilpert *et al.*, 2016 deepTools2: a next generation web server for deep-sequencing data analysis. Nucleic Acids Res 44: W160-165.
Rhoades, A. R., S. Ruone and T. Formosa, 2004 Structural features of nucleosomes reorganized by yeast FACT and its HMG box component, Nhp6. Mol Cell Biol 24: 3907-3917.
Ruone, S., A. R. Rhoades and T. Formosa, 2003 Multiple Nhp6 molecules are required to recruit Spt16-Pob3 to form yFACT complexes and to reorganize nucleosomes. J Biol Chem 278: 45288-45295.
Safina, A., P. Cheney, M. Pal, L. Brodsky, A. Ivanov *et al.*, 2017 FACT is a sensor of DNA torsional stress in eukaryotic cells. Nucleic Acids Res 45: 1925-1945.

Saunders, A., J. Werner, E. D. Andrulis, T. Nakayama, S. Hirose *et al.*, 2003 Tracking FACT and the RNA polymerase II elongation complex through chromatin in vivo. Science 301**:** 1094-1096.

Schlesinger, M. B., and T. Formosa, 2000 POB3 is required for both transcription and replication in the yeast Saccharomyces cerevisiae. Genetics 155**:** 1593-1606.

Schwabish, M. A., and K. Struhl, 2004 Evidence for eviction and rapid deposition of histones upon transcriptional elongation by RNA polymerase II. Mol Cell Biol 24**:** 10111-10117.

Sen, R., A. Kaja, J. Ferdoush, S. Lahudkar, P. Barman *et al.*, 2017 An mRNA capping enzyme targets FACT to the active gene to enhance the engagement of RNA polymerase II into transcriptional elongation. Mol Cell Biol.

Sheinin, M. Y., M. Li, M. Soltani, K. Luger and M. D. Wang, 2013 Torque modulates nucleosome stability and facilitates H2A/H2B dimer loss. Nat Commun 4**:** 2579.

Simic, R., D. L. Lindstrom, H. G. Tran, K. L. Roinick, P. J. Costa *et al.*, 2003 Chromatin remodeling protein Chd1 interacts with transcription elongation factors and localizes to transcribed genes. EMBO J 22**:** 1846-1856.

Squazzo, S. L., P. J. Costa, D. L. Lindstrom, K. E. Kumer, R. Simic *et al.*, 2002 The Paf1 complex physically and functionally associates with transcription elongation factors in vivo. EMBO J 21**:** 1764-1774.

Stuwe, T., M. Hothorn, E. Lejeune, V. Rybin, M. Bortfeld *et al.*, 2008 The FACT Spt16 "peptidase" domain is a histone H3-H4 binding module. Proc Natl Acad Sci U S A 105**:** 8884-8889.

Tardiff, D. F., K. C. Abruzzi and M. Rosbash, 2007 Protein characterization of Saccharomyces cerevisiae RNA polymerase II after in vivo cross-linking. Proc Natl Acad Sci U S A 104**:** 19948-19953.

Tessarz, P., H. Santos-Rosa, S. C. Robson, K. B. Sylvestersen, C. J. Nelson *et al.*, 2014 Glutamine methylation in histone H2A is an RNA-polymerase-I-dedicated modification. Nature 505**:** 564-568.

Teves, S. S., and S. Henikoff, 2014 DNA torsion as a feedback mediator of transcription and chromatin dynamics. Nucleus 5**:** 211-218.

Travers, A. A., 2003 Priming the nucleosome: a role for HMGB proteins? EMBO Rep 4**:** 131-136.

True, J. D., J. J. Muldoon, M. N. Carver, K. Poorey, S. J. Shetty *et al.*, 2016 The Modifier of Transcription 1 (Mot1) ATPase and Spt16 Histone Chaperone Co-regulate Transcription through Preinitiation Complex Assembly and Nucleosome Organization. J Biol Chem 291**:** 15307-15319.

Tsunaka, Y., Y. Fujiwara, T. Oyama, S. Hirose and K. Morikawa, 2016 Integrated molecular mechanism directing nucleosome reorganization by human FACT. Genes Dev 30**:** 673-686.

Tsunaka, Y., J. Toga, H. Yamaguchi, S. Tate, S. Hirose *et al.*, 2009 Phosphorylated intrinsically disordered region of FACT masks its nucleosomal DNA binding elements. J Biol Chem 284**:** 24610-24621.

Ulyanova, N. P., and G. R. Schnitzler, 2005 Human SWI/SNF generates abundant, structurally altered dinucleosomes on polynucleosomal templates. Mol Cell Biol 25**:** 11156-11170.

Valieva, M. E., G. A. Armeev, K. S. Kudryashova, N. S. Gerasimova, A. K. Shaytan *et al.*, 2016 Large-scale ATP-independent nucleosome unfolding by a histone chaperone. Nat Struct Mol Biol 23**:** 1111-1116.

Valieva, M. E., N. S. Gerasimova, K. S. Kudryashova, A. L. Kozlova, M. P. Kirpichnikov *et al.*, 2017 Stabilization of Nucleosomes by Histone Tails and by FACT Revealed by spFRET Microscopy. Cancers (Basel) 9.

VanDemark, A. P., M. Blanksma, E. Ferris, A. Heroux, C. P. Hill *et al.*, 2006 The structure of the yFACT Pob3-M domain, its interaction with the DNA replication factor RPA, and a potential role in nucleosome deposition. Mol Cell 22**:** 363-374.

VanDemark, A. P., H. Xin, L. McCullough, R. Rawlins, S. Bentley *et al.*, 2008 Structural and functional analysis of the Spt16p N-terminal domain reveals overlapping roles of yFACT subunits. J Biol Chem 283**:** 5058-5068.

Vasseur, P., S. Tonazzini, R. Ziane, A. Camasses, O. J. Rando *et al.*, 2016 Dynamics of Nucleosome Positioning Maturation following Genomic Replication. Cell Rep.

Vinayachandran, V., R. Reja, M. J. Rossi, B. Park, L. Rieber *et al.*, 2018 Widespread and precise reprogramming of yeast protein-genome interactions in response to heat shock. Genome Res.

Voth, W. P., S. Takahata, J. L. Nishikawa, B. M. Metcalfe, A. M. Naar *et al.*, 2014 A role for FACT in repopulation of nucleosomes at inducible genes. PLoS One 9**:** e84092.

Wang, T., Y. Liu, G. B. Edwards, D. D. Krzizike, H. Scherman *et al.*, 2018.

Warfield, L., S. Ramachandran, T. Baptista, D. Devys, L. Tora *et al.*, 2017 Transcription of Nearly All Yeast RNA Polymerase II-Transcribed Genes Is Dependent on Transcription Factor TFIID. Mol Cell.

Winkler, D. D., U. M. Muthurajan, A. R. Hieb and K. Luger, 2011 Histone chaperone FACT coordinates nucleosome interaction through multiple synergistic binding events. J Biol Chem 286**:** 41883-41892.

Wittmeyer, J., and T. Formosa, 1997 The Saccharomyces cerevisiae DNA polymerase alpha catalytic subunit interacts with Cdc68/Spt16 and with Pob3, a protein similar to an HMG1-like protein. Mol Cell Biol 17**:** 4178-4190.

Wong, K. H., Y. Jin and K. Struhl, 2014 TFIIH phosphorylation of the Pol II CTD stimulates mediator dissociation from the preinitiation complex and promoter escape. Mol Cell 54**:** 601-612.

Xin, H., S. Takahata, M. Blanksma, L. McCullough, D. J. Stillman *et al.*, 2009 yFACT induces global accessibility of nucleosomal DNA without H2A-H2B displacement. Mol Cell 35**:** 365-376.

Yang, J., X. Zhang, J. Feng, H. Leng, S. Li *et al.*, 2016 The Histone Chaperone FACT Contributes to DNA Replication-Coupled Nucleosome Assembly. Cell Rep.

Zhang, Z., C. J. Wippo, M. Wal, E. Ward, P. Korber *et al.*, 2011 A packing mechanism for nucleosome organization reconstituted across a eukaryotic genome. Science 332**:** 977-980.

Zheng, S., J. B. Crickard, A. Srikanth and J. C. Reese, 2014 A highly conserved region within H2B is important for FACT to act on nucleosomes. Mol Cell Biol 34**:** 303-314.

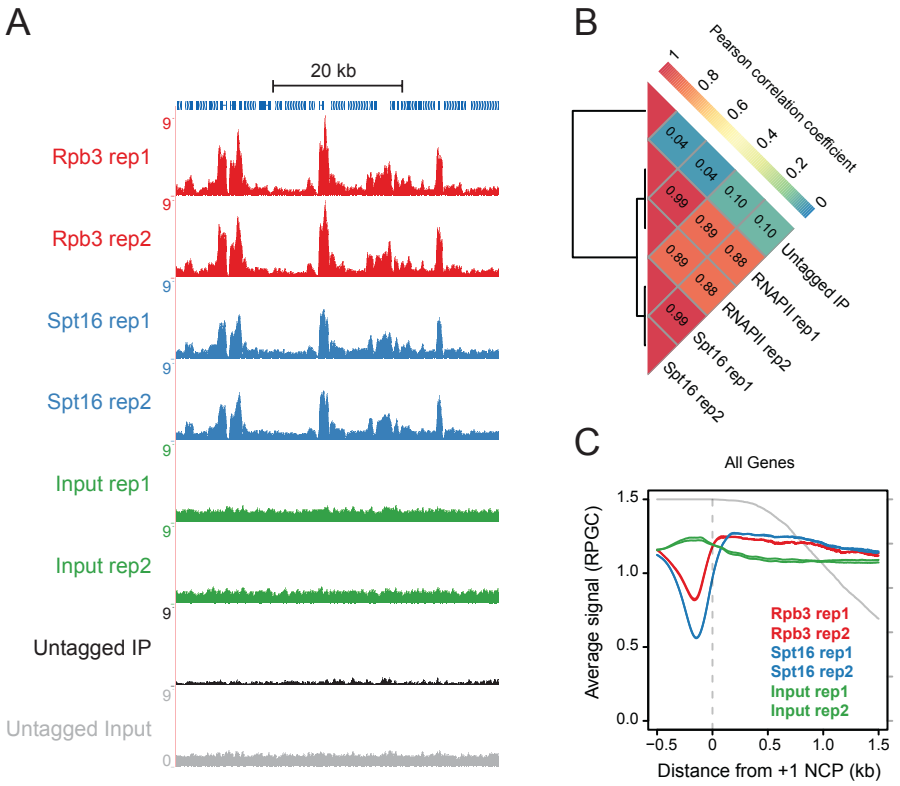

Figure 1: FACT and RNAPII co-localize. A) Genome browser tracks of sequence coverage (RPGC) from Rpb3 and Spt16 ChIP from sonicated chromatin (Input) and an untagged control over chrIV 300,000 - 350,000. The untagged IP was scaled by using spike-in exogenous DNA (see methods). B) Pearson correlation matrix for sequence coverage of Spt16, Rpb3 and untagged IPs across genome-wide 250bp bins. C) The average Rpb3, Spt16, and sonicated input sequence coverage (RPGC) relative to the +1 NCP of 5521 genes.

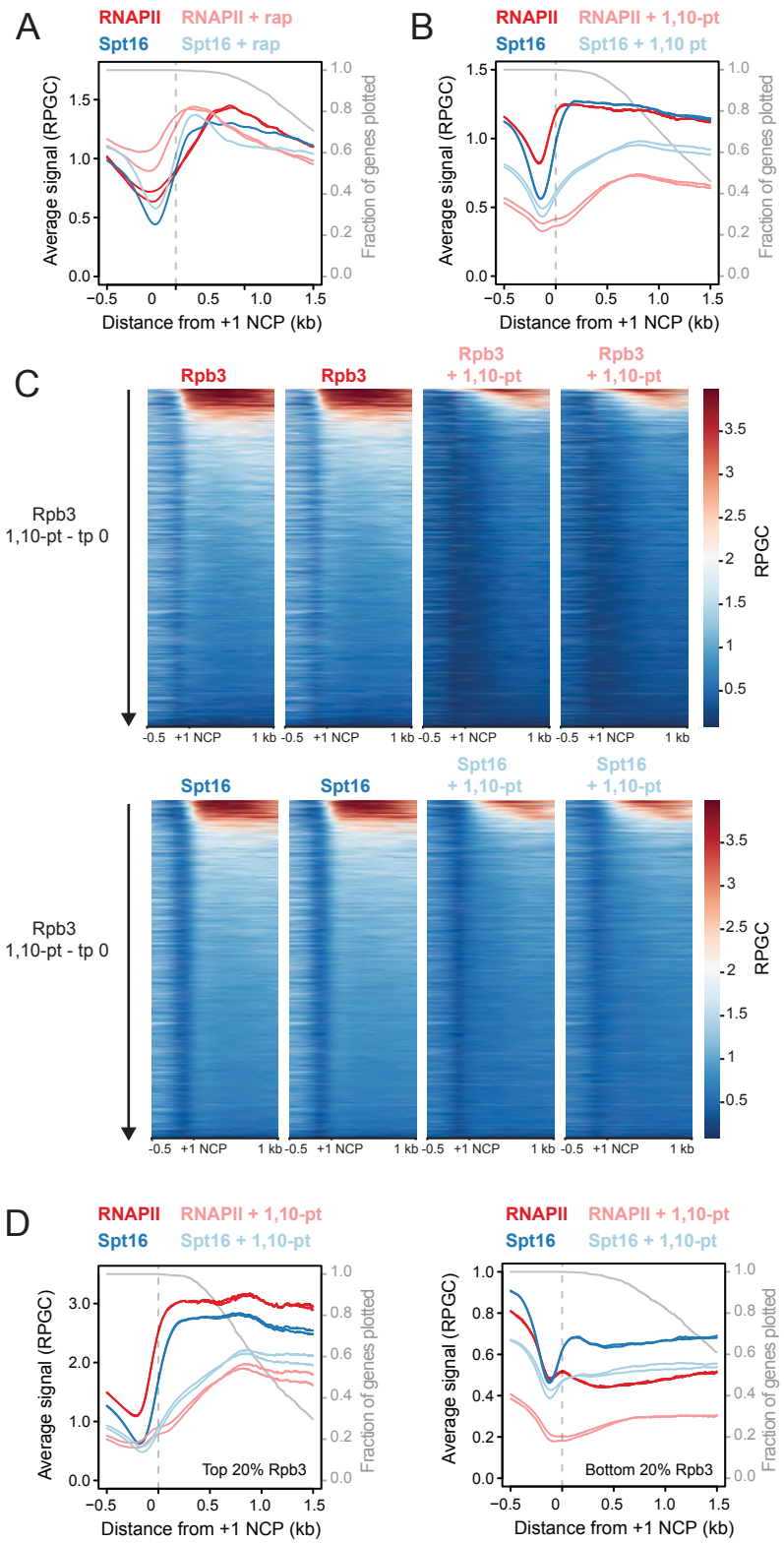

Figure 2: The interaction of FACT with chromatin is dependent on transcription. A) Rpb3 and Spt16 sequence coverage (RPGC), from cells expressing Kin28 with an FRB tag that was "anchored away" in the presence of rapamycin (rap), relative to the +1 NCP of 5521 genes. B) As in (A) except from cells with and without treatment with 1,10-phenanthroline (1,10-pt). Fragment coverage was normalized using "spiked-in" control DNA. C) Rpb3 and Spt16 sequence coverage (RPGC) relative to 5521 +1 NCPs (Chereji et al. 2018) prior to or following 15 minute treatment with 1,10-pt, represented by heatmap. D) As in (B) but for the top and bottom 20% of transcribed genes (1105 genes), as determined by Rpb3 binding.

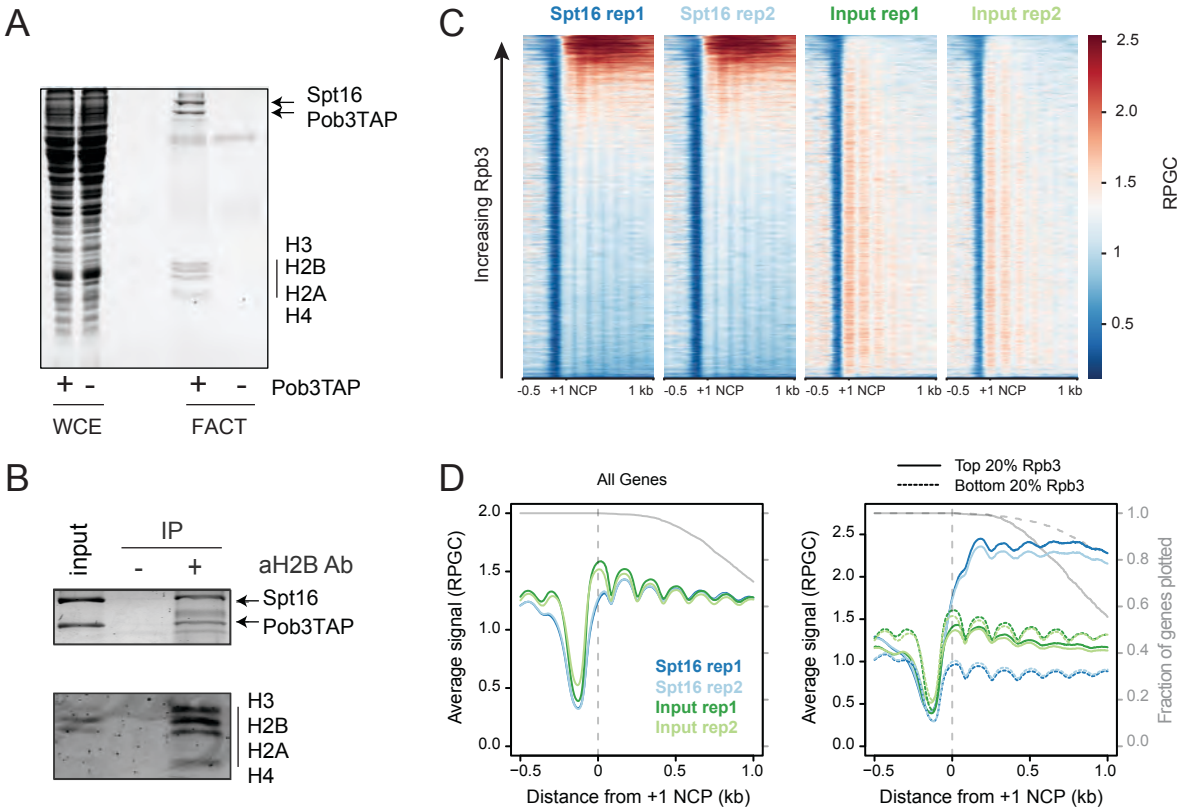

Figure 3: FACT binds nucleosomes in vivo. A) FACT, purified from a strain expressing TAP-tagged Pob3 (+), was subjected to SDS PAGE analysis with coomassie staining. And untagged strain (-) was used as a negative control. B) FACT and associated histones were purified from whole cell extracts via a TAP tag on Pob3. Purified FACT was eluted, by cleavage of the TAP tag with TEV protease, and subjected to immunoprecipitation with antibodies specific for H2B. The proteins in input and immunoprecipitated fractions were visualized by coomassie staining of an SDS PAGE gel. C) Spt16 and MNase input sequence coverage (RPGC) relative to 5521 +1 NCPs (Chereji et al. 2018) represented by heatmap. D) As in (C), but data represented as the average sequence coverage (RPGC) overlapping 5521 +1 NCPs and the top and bottom 20% of Rpb3 bound genes (1105 genes each).

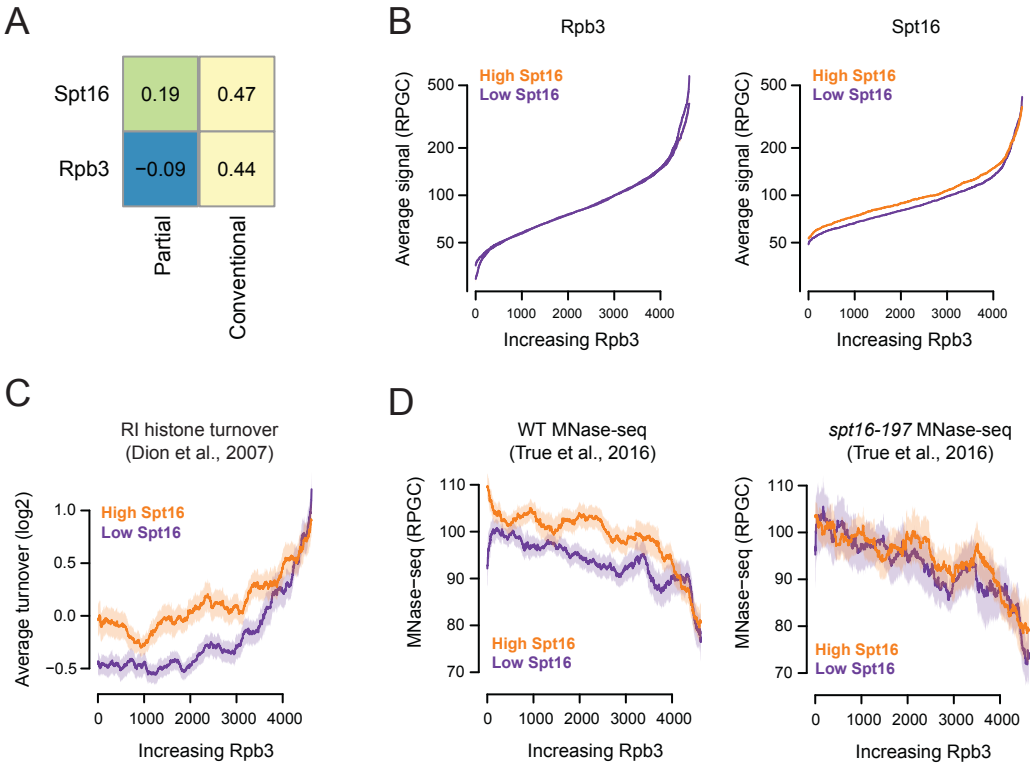

Figure 4: FACT co-localizes with RI histone turnover independently of RNAPII. A) Gene-based conventional and partial Spearman correlation coefficients represented by heatmap. B) Genes, as in (A), were ordered by Rpb3 levels and in 500 gene sliding windows the top and bottom 20% of Spt16-Rpb3 were designated as high and low Spt16 groups. Mean enrichment of Rpb3, Spt16 are plotted with the shaded region representing the 95% confidence interval. C,D) Using the same gene windows as in (B), RI histone turnover (Dion et al., 2007) (C) and MNase-seq coverage from wildtype and spt16-197 strains following 45 minute shift to the restrictive temperature (D) are plotted with the shaded region representing the 95% confidence interval.

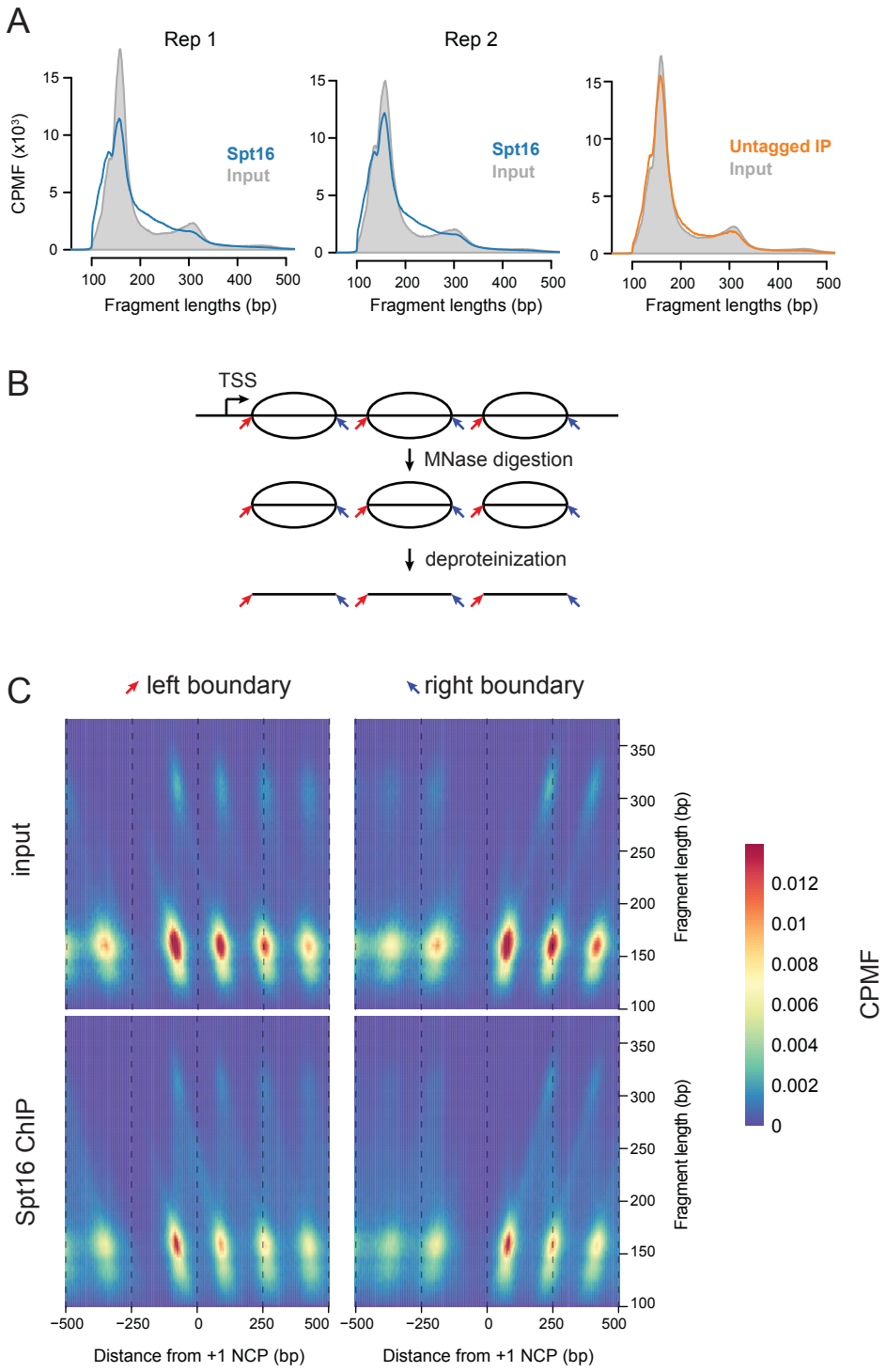

Figure 5: FACT-bound nucleosomes exhibit altered MNase sensitivity A) Histograms depicting DNA fragment lengths recovered from input, Spt16-6HA, and untagged control ChIPs from MNase-digested chromatin B) Designation of left (red arrows) and right (blue arrows) nucleosome fragment boundaries identified through MNase digestion of chromatin. C) Two dimensional plots of positions of nucleosome boundaries in input and Spt16 ChIP from MNase digested chromatin, relative to the +1 nucleosome of 5521 annotated genes in S. cerevisiae. the sum of fragment boundary counts are indicated as a heatmap, the sequence fragment lengths (split into 3 bp bins) is plotted ont he Y-axis and the position of nucleosome boundaries relative to the +1 nucleosome is plotted on the X-axis.

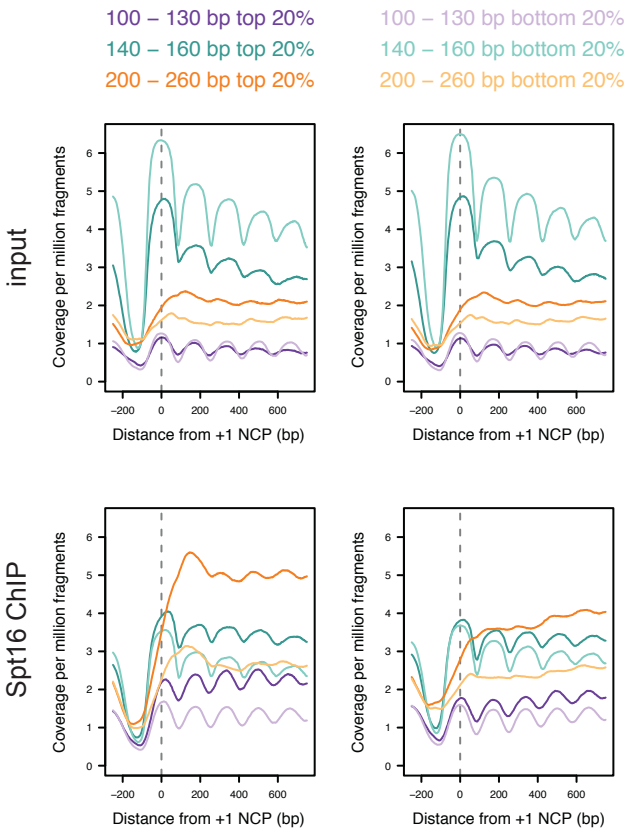

Figure 6: Transcription enhances nuclease senstivity of FACT-bound nucleosomes. MNase input and Spt16 ChIP-seq sequence for cells with and without treatment with 1,10-pt, relative to the +1 NCP of the top and bottom 20% of transcribed genes (1105 genes each). Sequence fragments were selected and coverage per million fragments (of all sizes) is plotted.

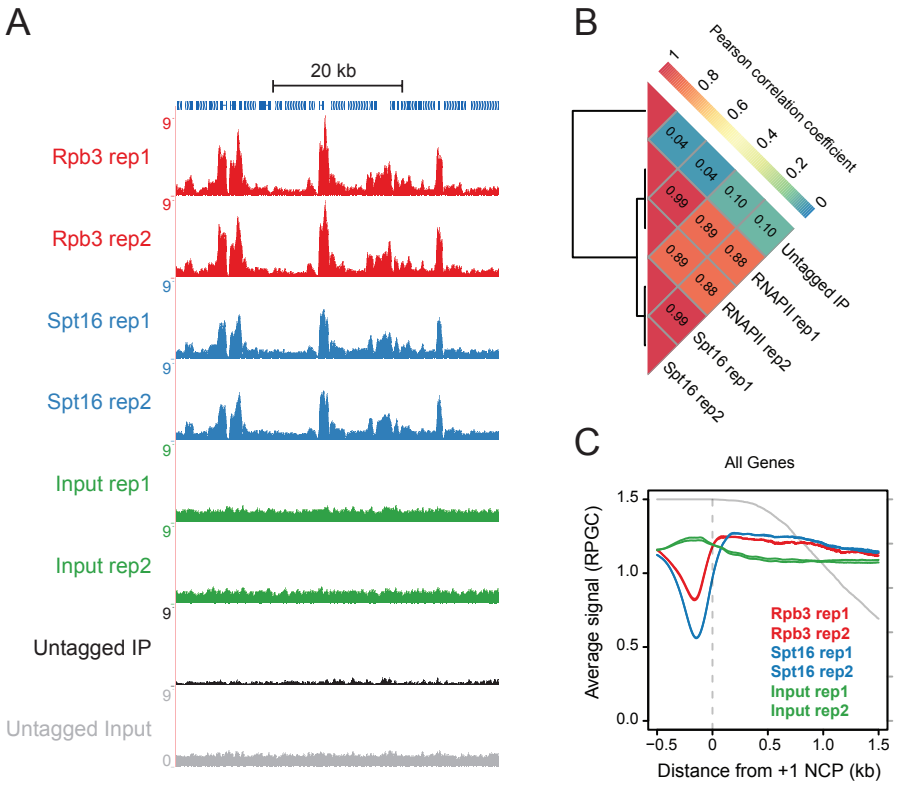

Figure 1: FACT and RNAPII co-localize. A) Genome browser tracks of sequence coverage (RPGC) from Rpb3 and Spt16 ChIP from sonicated chromatin (Input) and an untagged control over chrIV 300,000 - 350,000. The untagged IP was scaled by using spike-in exogenous DNA (see methods). B) Pearson correlation matrix for sequence coverage of Spt16, Rpb3 and untagged IPs across genome-wide 250bp bins. C) The average Rpb3, Spt16, and sonicated input sequence coverage (RPGC) relative to the +1 NCP of 5521 genes.

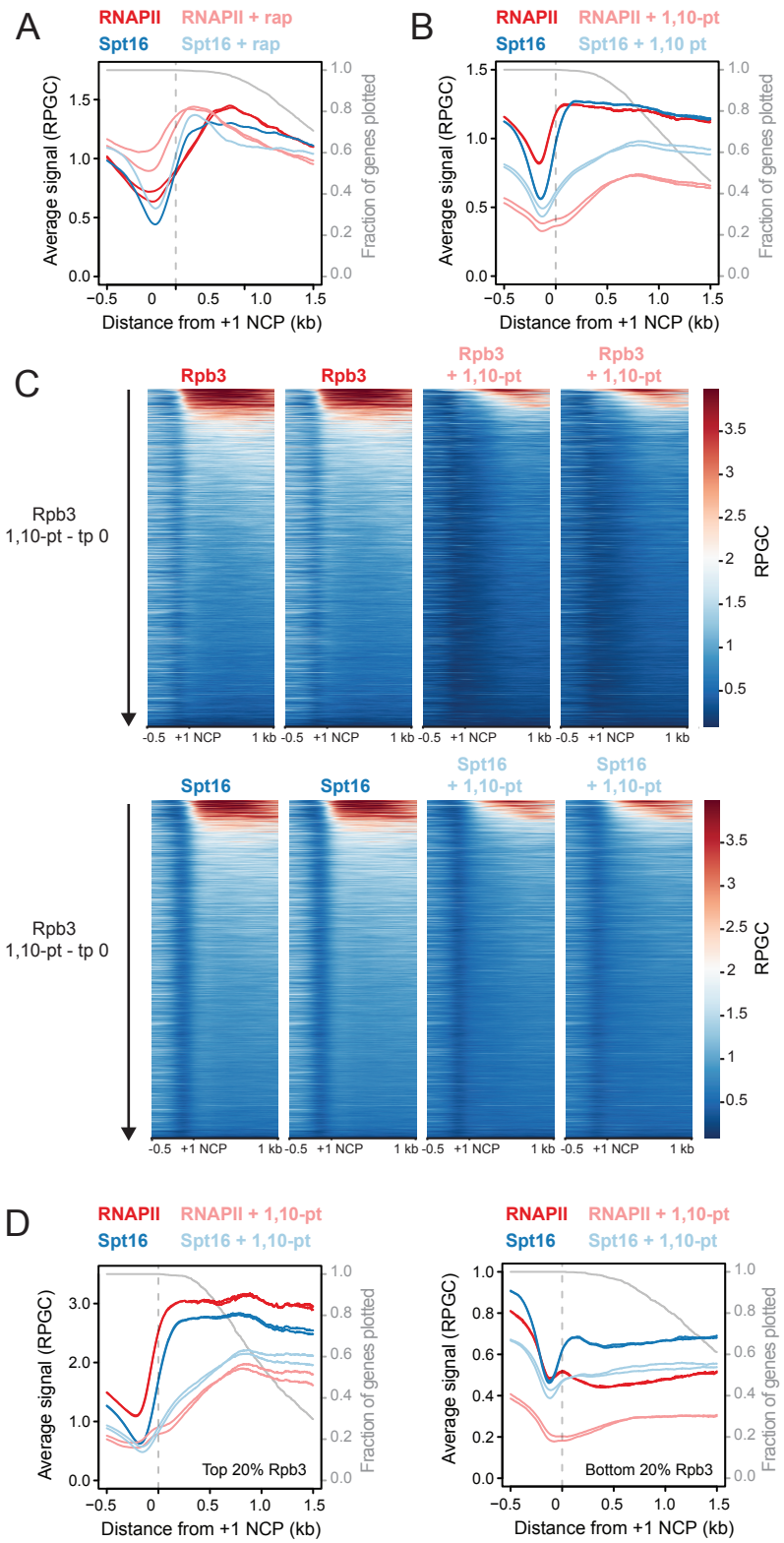

Figure 2: The interaction of FACT with chromatin is dependent on transcription. A) Rpb3 and Spt16 sequence coverage (RPGC), from cells expressing Kin28 with an FRB tag that was "anchored away" in the presence of rapamycin (rap), relative to the +1 NCP of 5521 genes. B) As in (A) except from cells with and without treatment with 1,10-phenanthroline (1,10-pt). Fragment coverage was normalized using "spiked-in" control DNA. C) Rpb3 and Spt16 sequence coverage (RPGC) relative to 5521 +1 NCPs (Chereji et al. 2018) prior to or following 15 minute treatment with 1,10-pt, represented by heatmap. D) As in (B) but for the top and bottom 20% of transcribed genes (1105 genes), as determined by Rpb3 binding.

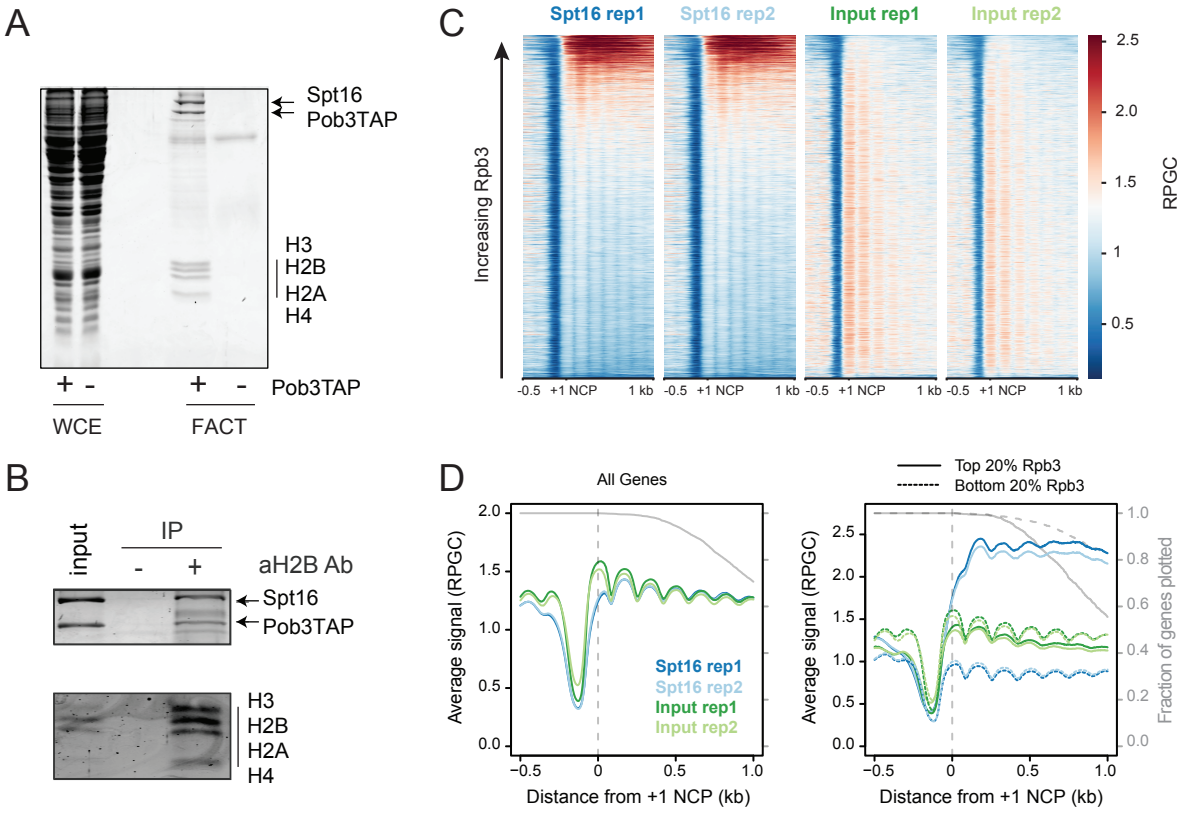

Figure 3: FACT binds nucleosomes in vivo. A) FACT, purified from a strain expressing TAP-tagged Pob3 (+), was subjected to SDS PAGE analysis with coomassie staining. And untagged strain (-) was used as a negative control. B) FACT and associated histones were purified from whole cell extracts via a TAP tag on Pob3. Purified FACT was eluted, by cleavage of the TAP tag with TEV protease, and subjected to immunoprecipitation with antibodies specific for H2B. The proteins in input and immunoprecipitated fractions were visualized by coomassie staining of an SDS PAGE gel. C) Spt16 and MNase input sequence coverage (RPGC) relative to 5521 +1 NCPs (Chereji et al. 2018) represented by heatmap. D) As in (C), but data represented as the average sequence coverage (RPGC) overlapping 5521 +1 NCPs and the top and bottom 20% of Rpb3 bound genes (1105 genes each).

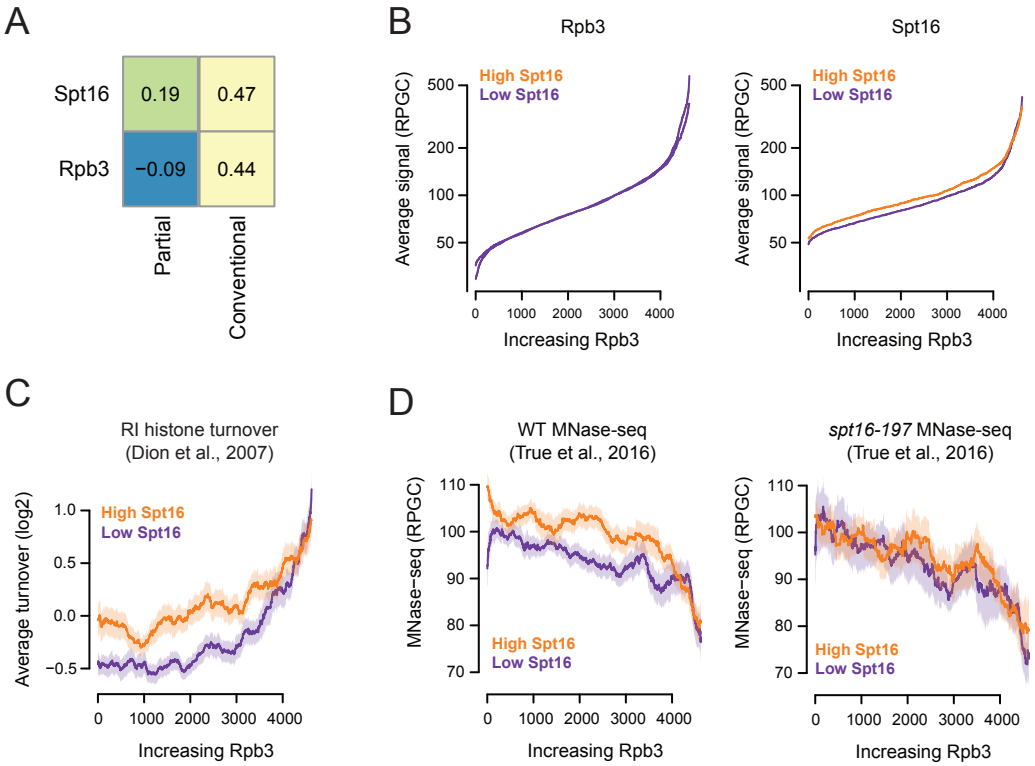

Figure 4: FACT co-localizes with RI histone turnover independently of RNAPII. A) Gene-based conventional and partial Spearman correlation coefficients represented by heatmap. B) Genes, as in (A), were ordered by Rpb3 levels and in 500 gene sliding windows the top and bottom 20% of Spt16-Rpb3 were designated as high and low Spt16 groups. Mean enrichment of Rpb3, Spt16 are plotted with the shaded region representing the 95% confidence interval. C,D) Using the same gene windows as in (B), RI histone turnover (Dion et al., 2007) (C) and MNase-seq coverage from wildtype and spt16-197 strains following 45 minute shift to the restrictive temperature (D) are plotted with the shaded region representing the 95% confidence interval.

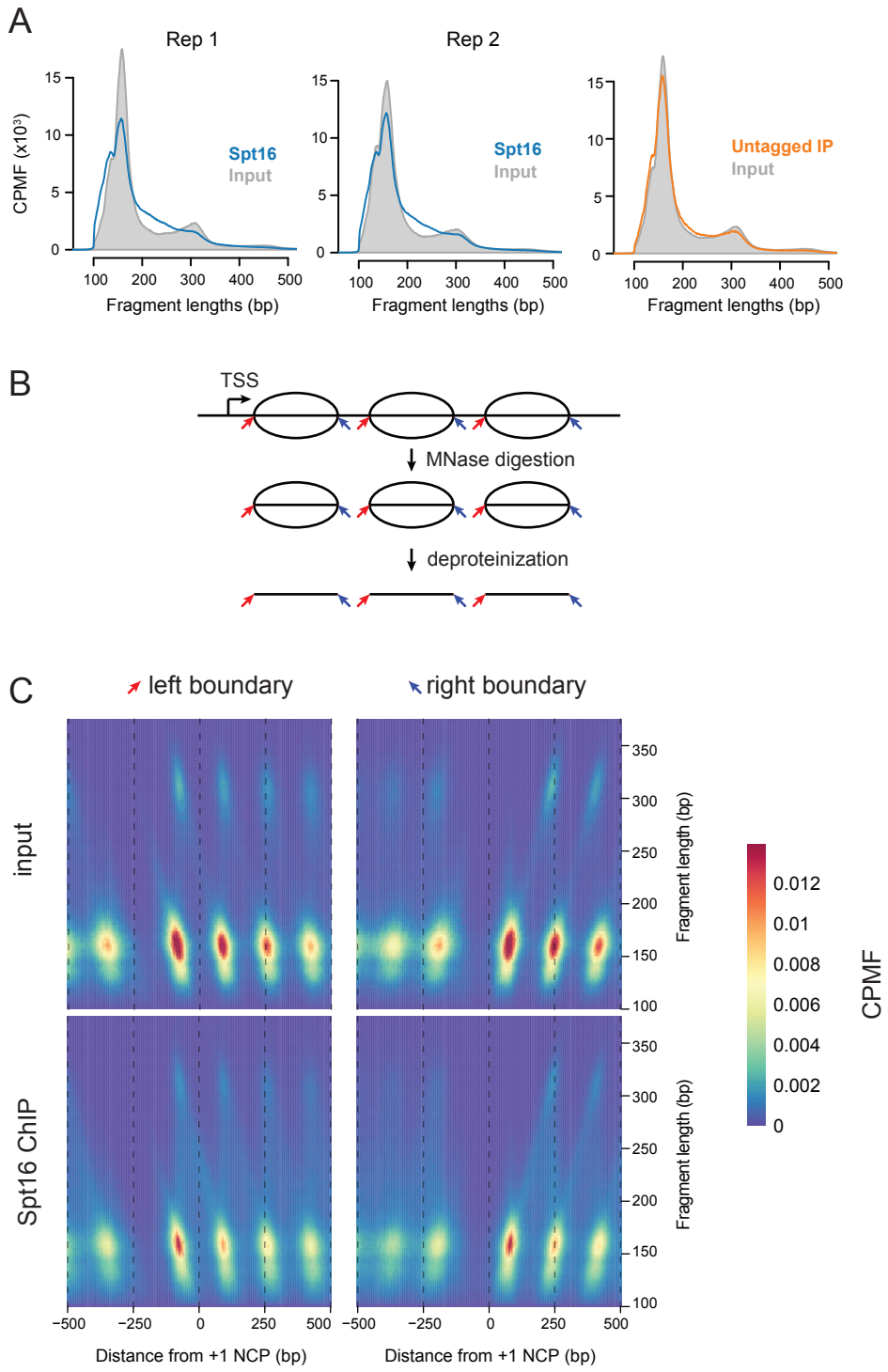

Figure 5: FACT-bound nucleosomes exhibit altered MNase sensitivity A) Histograms depicting DNA fragment lengths recovered from input, Spt16-6HA, and untagged control ChIPs from MNase-digested chromatin B) Designation of left (red arrows) and right (blue arrows) nucleosome fragment boundaries identified through MNase digestion of chromatin. C) Two dimensional plots of positions of nucleosome boundaries in input and Spt16 ChIP from MNase digested chromatin, relative to the +1 nucleosome of 5521 annotated genes in S. cerevisiae. the sum of fragment boundary counts are indicated as a heatmap, the sequence fragment lengths (split into 3 bp bins) is plotted ont he Y-axis and the position of nucleosome boundaries relative to the +1 nucleosome is plotted on the X-axis.

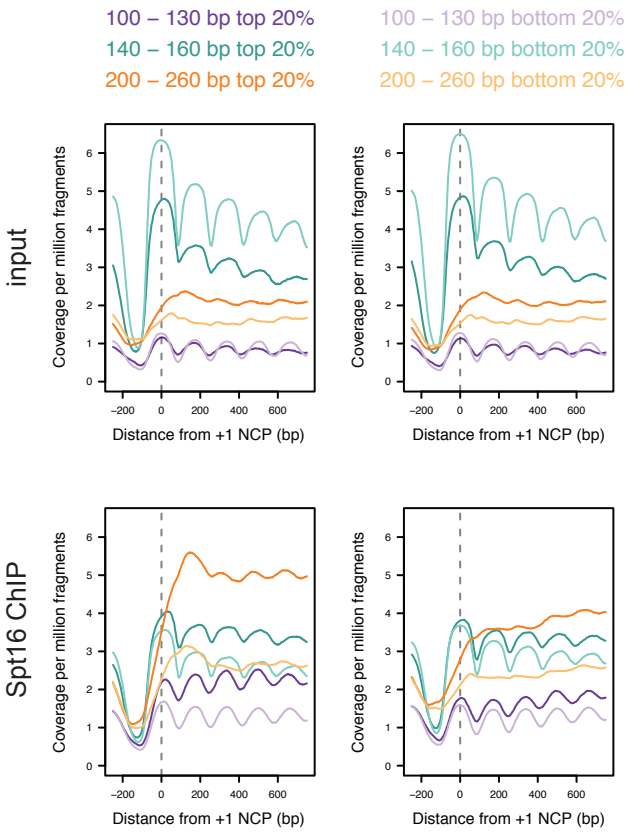

Figure 6: Transcription enhances nuclease senstivity of FACT-bound nucleosomes. MNase input and Spt16 ChIP-seq sequence for cells with and without treatment with 1,10-pt, relative to the +1 NCP of the top and bottom 20% of transcribed genes (1105 genes each). Sequence fragments were selected and coverage per million fragments (of all sizes) is plotted.

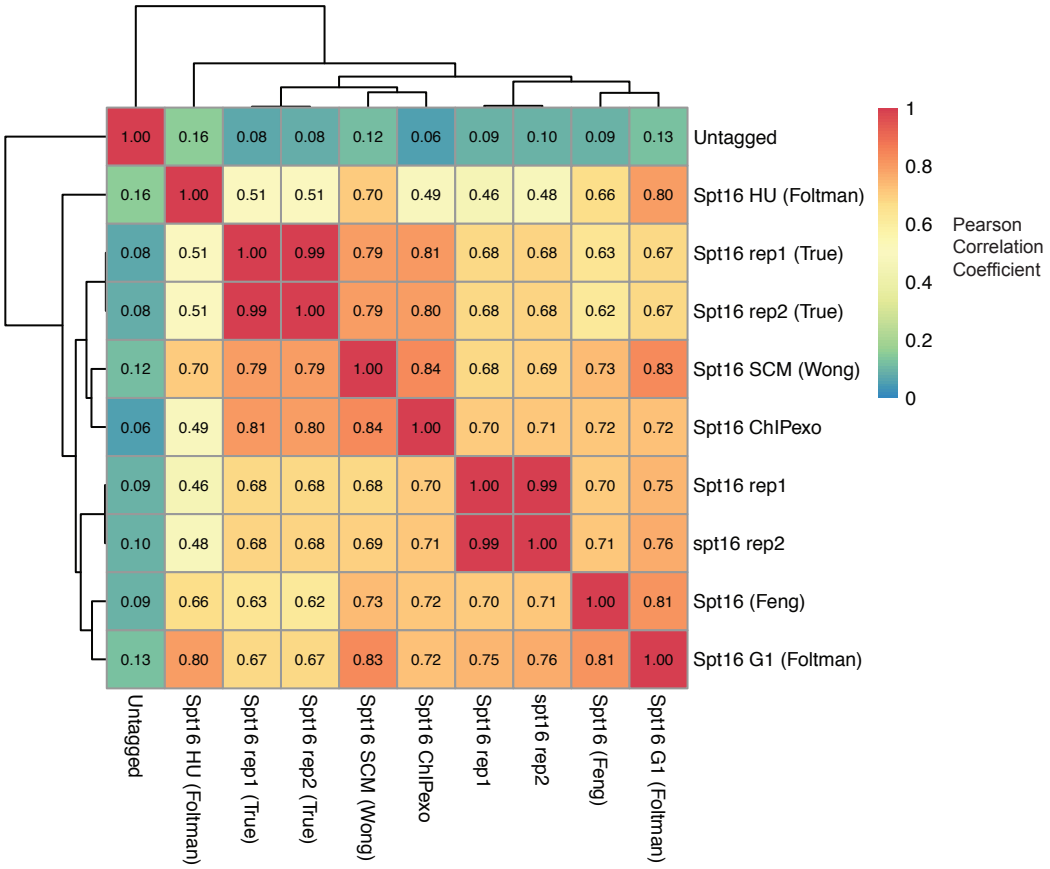

Figure S1: Comparison of Spt16 ChIPs. Pearson correlation matrix for sequence coverage of our Spt16 and untagged IPs, with previously published Spt16 ChIP-seq and ChIP-exo experiments, across genome-wide 250bp bins.

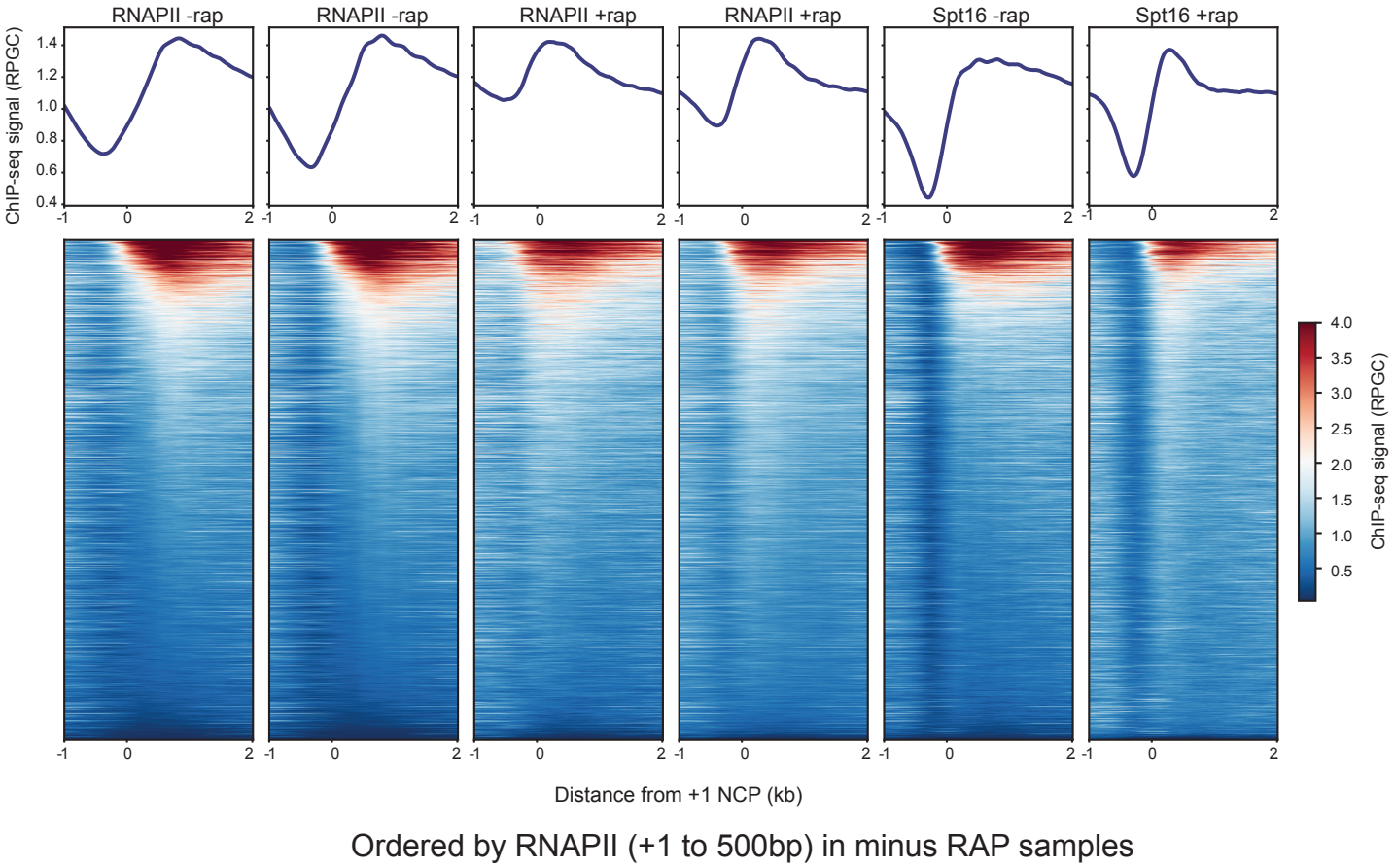

Figure S2: Change in RNAPII and Spt16 following depletion of TFIIH. RNAPII and Spt16 sequence coverage (RPGC) relative to 5521 +1 NCPs, ordered by RNAPII signal (in first 500bp) in untreated samples and represented by heatmap.

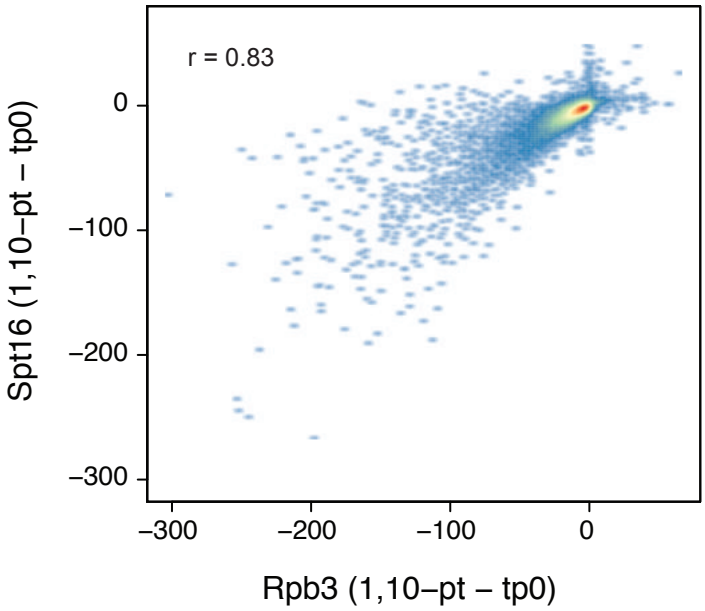

Figure S3: Genome wide changes in Spt16 and RNAPII following transcription inhibition. ChIP-seq fragment midpoint counts per million fragments, in 250 bp genome wide windows, showing the change in Rpb3 and Spt16 following transcription inhibition by smoothed scatter plot. Pearson correlation coefficient indicated as ‘r’.

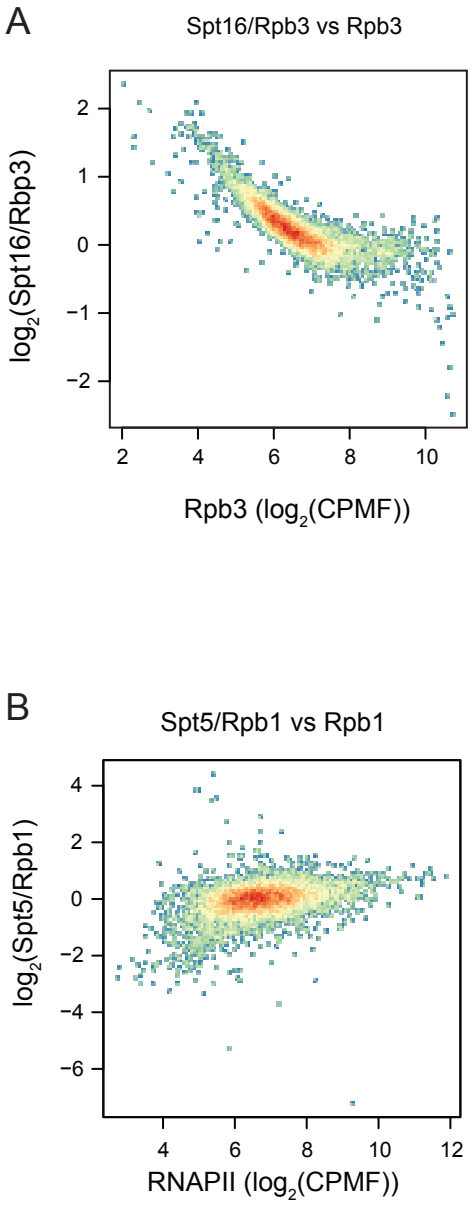

Figure S4: Increased FACT binding relative to RNAPII at lowly transcribed genes. A. Smoothed scatter plot of Rpb3 and Spt16/Rpb3 across gene bodies. CPMF: Counts Per Million Fragments per Kb. B. As in A, but for Spt5 and Rpb1.

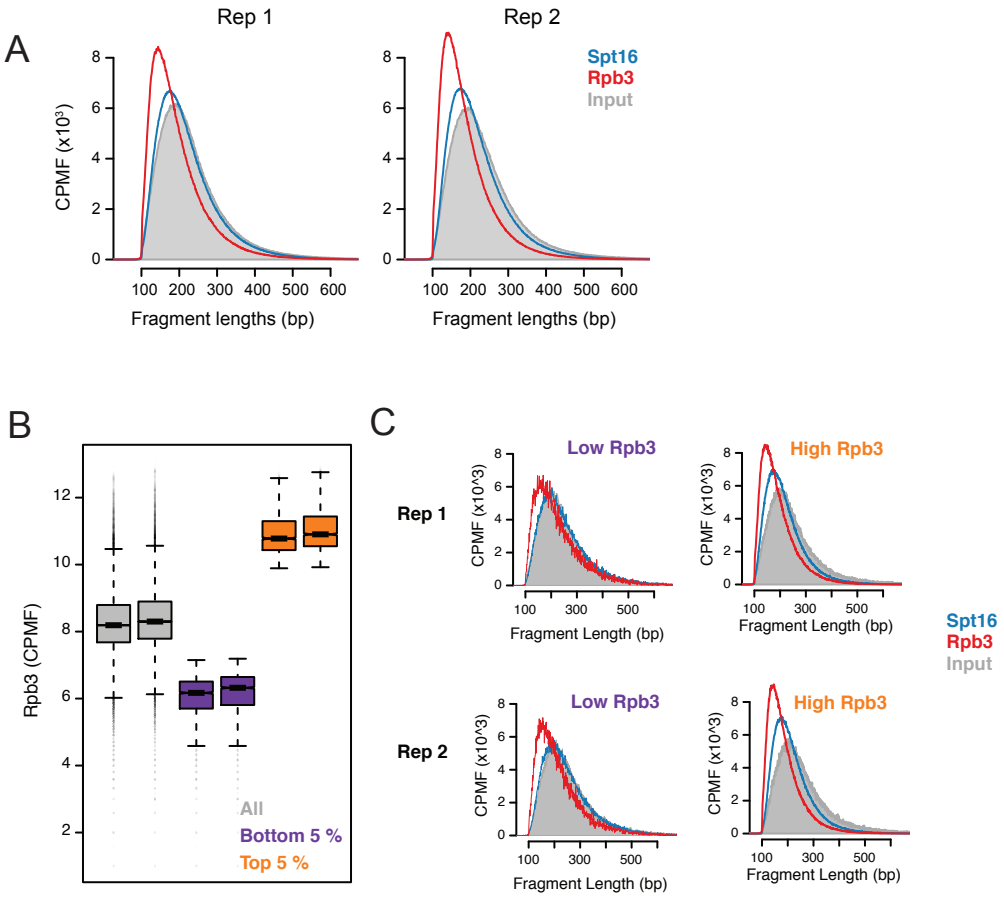

Figure S5: Rpb3 and Spt16 differences in fragment lengths of ChIP-seq DNA. A) Histograms depicting DNA fragment lengths recovered from input, Spt16-6HA, and Rpb3 ChIPs from sonicated chromatin. B) Rpb3 levels in 250 bp genome-wide bins, depicted by boxplots, for all, the top 5% of Rpb3 bound bins, and the bottom 5% of Rpb3 bound bins. C) Histograms depicting DNA fragment lengths recovered from input, Spt16-6HA, and Rpb3 ChIPs from sonicated chromatin, for fragments overlapping the top and bottom 5% of Rpb3-bound 250 bp genome wide bins.

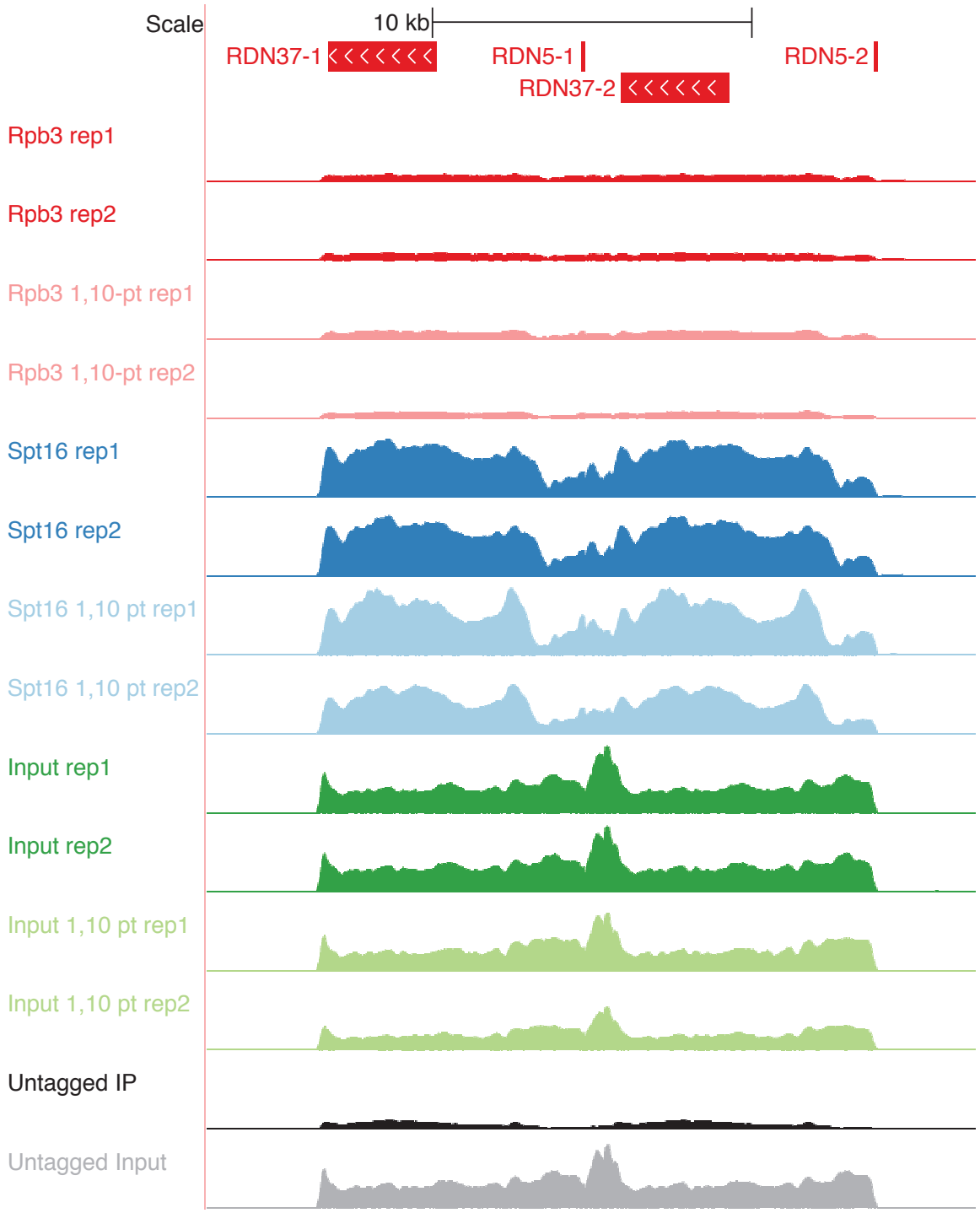

Figure S6: The interaction of FACT with RNAPI-transcribed regions is dependent on transcription. Genome browser screenshot of sequence read counts, normalized to sonicated chromatin (input), from Rpb3 and Spt16 chromatin immunoprecipitation (IP) over chrXII 448000-472000. The position of two 35S (RDN37) and 5S (RDN5) rDNA genes repeats are indicated. Datasets were normalized to genomic mean and samples from 1,10-phenanthroline-treated cells (1,10 pt) were further normalized to data from untreated cells based on spike-in controls.

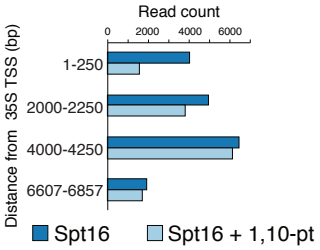

Figure S7. The interaction of FACT with RNAPI-transcribed regions is dependent on transcription. “Spike-in” normalized Spt16 ChIP-seq read counts from cells with and without treatment with 1,10-phenanthroline (1,10-pt) over the indicated bins relative to the TSS of the 35S rRNA genes were plotted.

Figure S8: The interaction of FACT with RNAPIII-transcribed regions is dependent on transcription. Genome browser screenshots of ChIP-chip data, normalized to sonicated chromatin (input), for the indicated proteins over chrII 226000-228500 (left panel), chrVII 114500-117000.(middle panel) and chrXVI 688500-691000 (right panel). tRNA genes are indicated in red. Datasets were normalized to genomic mean and samples from 1,10-phenanthroline-treated (1,10 pt) cells were further normalized to data from untreated cells based on spike-in controls.

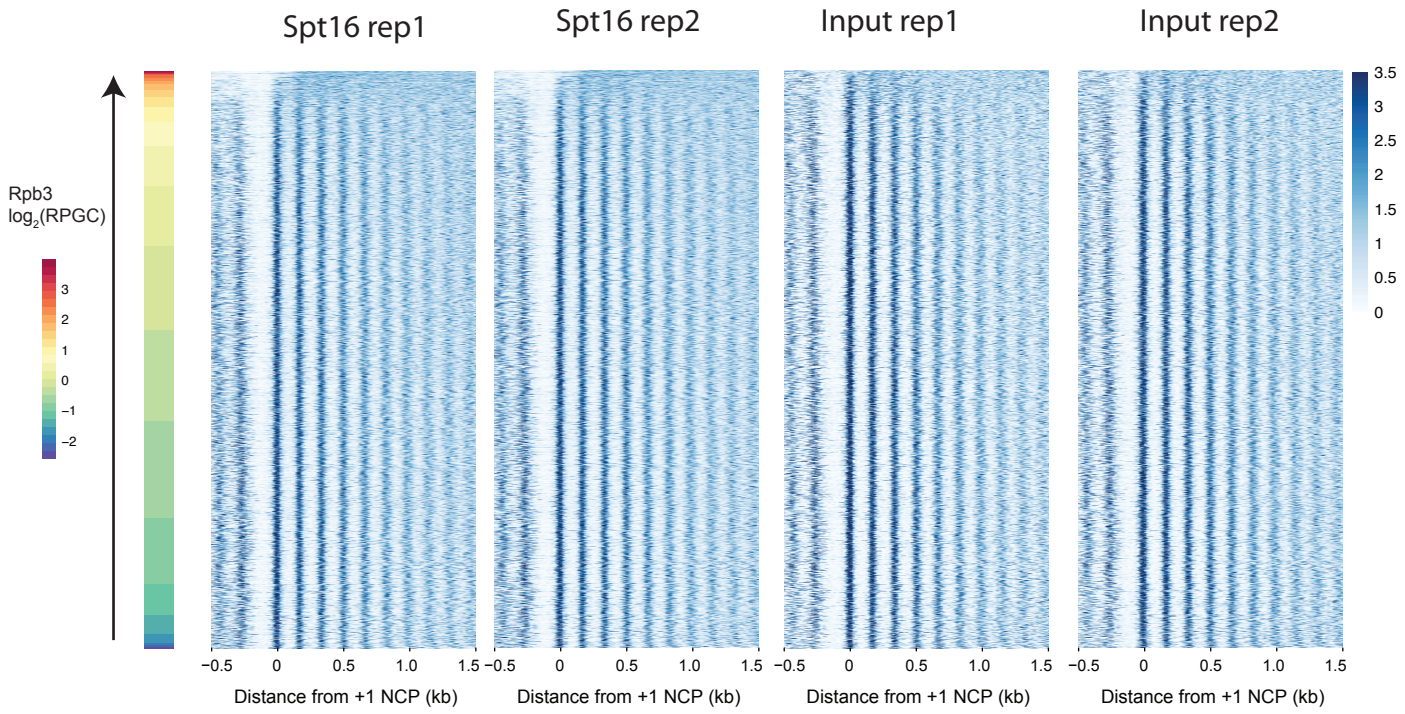

Figure S9: FACT-bound nucleosome positioning closely matches that of input nucleosome. Spt16 and MNase input dyad coverage (RPGC), for fragments from 100 bp to 200 bp in length, relative to +1 NCP of 2547 genes longer than 1500 bp (+1 NCP to TTS), ordered by RNAPII signal (in first 500bp) represented by row-normalized heatmap. Data represents the middle 3 bp for each fragment from 100 bp to 200 bp in length, to give an approximation of the nucleosome dyad positions. Each row is normalized by the mean signal, to give a row-normalized heatmap, and dyad distribution was smoothed by fitting to a smoothing spline.